Sea surface temperature variability in the central-western Mediterranean Sea during the last 2700 years: a multi-proxy and multi-record approach

M. Cisneros[1], I. Cacho[1], J. Frigola[1], M. Canals[1], P. Masqué[2,3,4], B. Martrat[5], M. Casado[5], J. Grimalt[5], G. Margaritelli[6] and F. Lirer[6]

[1] GRC Geociències Marines, Departament de Dinàmica de la Terra i l'Oceà, Facultat de Geologia, Universitat de Barcelona, Barcelona, Spain

[2] Institut de Ciència i Tecnologia Ambientals & Departament de Física, Universitat Autònoma de Barcelona, Bellaterra, Spain

[3] School of Natural Sciences and Centre for Marine Ecosystems Research, Edith Cowan University, Joondalup, Australia

[4] Oceans Institute and School of Physics, The University of Western Australia, Crawley, Australia

[5] Institut de Diagnosi Ambiental i Estudis de l'Aigua, Consell Superior d'Investigacions Científiques, Barcelona, Spain

[6] Istituto per l'Ambiente Marino Costiero (IAMC)–Consiglio Nazionale delle Ricerche, Calata Porta di Massa, Interno Porto di Napoli, 80133, Napoli, Italy

Correspondence to: M. Cisneros (mbermejo@ub.edu)

ABSTRACT

This study analyses the evolution of sea surface conditions during the last 2700 years in the central-western Mediterranean Sea based on six records as measured on five short sediment cores from two sites north of Minorca (cores MINMC06 and HER-MC-MR3). Sea Surface Temperatures (SSTs) were obtained from alkenones and *Globigerina bulloides*-Mg/Ca ratios combined with $\delta^{18}O$ measurements to reconstruct changes in the regional Evaporation–Precipitation (E–P) balance. We reviewed the *G. bulloides* Mg/Ca-SST calibration and re-adjusted it based on a set of core top measurements from the western Mediterranean Sea. According to the regional oceanographic data, the estimated Mg/Ca-SSTs are interpreted to reflect spring seasonal conditions mainly related to the April–May primary productivity bloom. In contrast, the Alkenone-SSTs signal likely integrates the averaged annual signal.

A combination of chronological tools allowed synchronizing the records in a common age model. Subsequently a single anomaly stack record was constructed for each proxy, thus easing to identify the most significant and robust patterns. The warmest SSTs occurred during the Roman Period (RP), which was followed by a general cooling trend interrupted by several centennial-scale oscillations. This general cooling trend could be controlled by changes in the annual mean insolation. Whereas some particularly warm SST intervals took place during the Medieval Climate Anomaly (MCA) the Little Ice Age (LIA) was markedly unstable with some very cold SST events mostly during its second half. The records of the last centuries suggest that relatively low E–P ratios and cold SSTs dominated during negative North Atlantic Oscillation (NAO) phases, although SST records seem to present a close positive connection with the Atlantic Multidecadal Oscillation index (AMO).

1 Introduction

The Mediterranean is regarded as one of the world's highly vulnerable regions with regard to the current global warming situation (Giorgi, 2006). This high sensitivity to climate variability has been evidenced in several studies focussed in past natural changes (Rohling et al., 1998; Cacho et al., 1999a; Moreno et al., 2002; Martrat et al., 2004; Reguera, 2004; Frigola et al., 2007; Combourieu Nebout et al., 2009). Paleo-studies focussed mostly in the rapid climate variability of the last glacial period have presented solid evidences of a tied connection between changes in North Atlantic oceanography and climate over the Western Mediterranean Region (Cacho et al., 1999b, 2000, 2001; Moreno et al., 2005; Sierro et al., 2005; Frigola et al., 2008; Fletcher and Sanchez-Goñi, 2008). Nevertheless, climate variability during the Holocene and, particularly during the last millennia, is not so well described in this region, although its understanding is crucial to place the nature of the 20th century trends in the recent climate history (Huang, 2004).

Some previous studies have already proposed that Holocene centennial climate variability in the western Mediterranean Sea could be linked to NAO variability (Jalut et al., 1997, 2000; Combourieu Nebout et al., 2002; Goy et al., 2003; Roberts et al., 2012; Fletcher et al., 2012). In particular, nine Holocene episodes of enhanced deep convection in the Gulf of Lion (GoL) and surface cooling conditions were described at the same location than this study (Frigola et al., 2007). These events have also been correlated to intensified upwelling conditions in the Alboran Sea and tentatively described as two-phase scenarios driven by distinctive NAO states (Ausín et al., 2015). A growing number of studies reveal considerable climate fluctuations during the last 2 kyr (Abrantes et al., 2005; Holzhauser et al., 2005; Kaufman et al., 2009; Lebreiro et al., 2006; Martín-Puertas et al., 2008; Kobashi et al., 2011; Nieto-Moreno et al., 2011, 2013; Moreno et al., 2012; PAGES 2K Consortium, 2013; Esper et al., 2014; McGregor et al., 2015). However, there is not uniformity about the exact time-span of the different defined climatic periods such for example the Medieval Climatic Anomaly (MCA), term coined originally by Stine (1994).

The existing Mediterranean climatic records for the last 1 or 2 kyr are mostly based on terrestrial source archives such as tree rings (Touchan et al., 2005, 2007; Griggs et al., 2007; Esper et al., 2007; Büntgen et al., 2011; Morellón et al., 2012), speleothem records (Frisia et al., 2003; Mangini et al., 2005; Fleitmann et al., 2009; Martín-Chivelet et al., 2011; Wassenburg et al., 2013), or lake reconstructions (Pla and Catalan, 2005; Martín-Puertas et al., 2008; Corella et al., 2011; Morellón et al., 2012). All of these archives can be good sensors of temperature and humidity changes but often their proxy records mix these two climate variables. Recent efforts have focussed in integrating these 2 kyr records into a regional climatic signals and they reveal a complexity in the regional response but also evidence the scarcity of marine records to have a more complete picture (PAGES, 2009; Lionello, 2012).

In reference to marine records, they are often limited by the lack of adequate time resolution and accurate chronology to produce detailed comparison with terrestrial source records, although they have the potential to provide a wider range of temperature sensitive proxies. Currently, few marine-source paleoclimate records are available from the last 2 kyr in the Mediterranean Sea (Schilman et al., 2001; Versteegh et al., 2007; Piva et al., 2008; Taricco et al., 2009, 2015; Incarbona et al., 2010; Fanget et al., 2012; Grauel et al., 2013; Lirer et al., 2013, 2014; Di Bella et al., 2014; Goudeau et al., 2015) and they are even more scarce in the Western Basin. The current disperse data is not enough to admit a potential commune pattern of marine Mediterranean climate variability for these two millennia (Taricco et al., 2009; Nieto-Moreno et al., 2011;

Moreno et al., 2012 and the references therein).

The aim of this study is to characterise changes in surface water properties from the Minorca margin in the Catalan-Balearic Sea (central-western Mediterranean), contributing to a better understanding of the climate variations in this region during the last 2.7 kyr. Sea Surface Temperature (SST) has been reconstructed by means of two independent proxies, Mg/Ca analyses on the planktonic foraminifera *Globigerina bulloides* and alkenone derived SST (Villanueva et al., 1997; Lea et al., 1999; Barker et al., 2005; Conte et al., 2006). The application of *G. bulloides*-Mg/Ca as a paleothermometer in the western Mediterranean Sea is tested through the analysis of a series of core top samples from different locations of the western Mediterranean Sea and the calibration reviewed consistently. Mg/Ca thermometry is applied with $\delta^{18}O$ in order to evaluate changes in the Evaporation–Precipitation (E–P) balance of the basin ultimately linked to salinity (Lea et al., 1999; Pierre, 1999; Barker et al., 2005). One of the limitations for the study of climate evolution of the last 2 kyr is that often the intensity of the climate oscillations is at the limit of detection of the selected proxies. In order to identify significant climatic patterns within the proxy records, the analysis have been performed in a collection of multicores from the same region, and their proxy records have been stacked. The studied time periods have been defined as follows (years expressed as BCE=Before Common Era and CE=Common Era): Talaiotic Period (TP; ending at 123 BCE); Roman Period (RP; from 123 BCE to 470 CE); Dark Middle Ages (DMA; from 470 until 900CE); Medieval Climate Anomaly (MCA; from 900 to 1275CE); Little Ice Age (LIA; from 1275 to 1850 CE) and Industrial Era (IE) as the most recent period. The limits of these periods are not uniform across the Mediterranean (Lionello, 2012) and here, the selected ages have been chosen according to historical events in Minorca Island and also to the classic climatic ones defined in literature (i.e.

Nieto-Moreno et al., 2011, 2013; Moreno et al., 2012; Lirer et al., 2013, 2014).

2 Climatic and oceanographic settings

The Mediterranean Sea is a semi-enclosed basin located in a transitional zone between different climate regimes, from the temperate zone at the north, to the subtropical zone at the south. Consequently, the Mediterranean climate is characterized by mild wet winters and warm to hot, dry summers (Lionello et al., 2006). Interannual climate variability is very much controlled by the dipole-like pressure gradient between the Azores (high) and Iceland (low) system known as the North Atlantic Oscillation (NAO) (Hurrell, 1995; Lionello and Sanna, 2005; Mariotti, 2011; Ausín et al., 2015). But the northern part of the Mediterranean region is also linked to other midlatitude teleconnection patterns (Lionello, 2012).

The Mediterranean Sea is a concentration basin (Béthoux, 1980; Lacombe et al., 1981) and the excess of evaporation with respect to freshwater input is balanced by water exchange at the Strait of Gibraltar (i.e. Pinardi and Masetti, 2000; Malanotte-Rizzoli et al., 2014). The basinwide circulation pattern is prevalently cyclonic (Millot, 1999). Three convection cells promote the Mediterranean deep and intermediate circulation: a basinwide open cell and two separated closed cells, one for the Western Basin and one for the Eastern part. The first one connects the two basins of the Mediterranean Sea though the Sicilia Strait, where water masses interchange occurs at intermediate depths. This cell is associated with the inflow of Atlantic Water (AW) at the Strait of Gibraltar and the outflow of the Levantine Intermediate Water (LIW) that flows below the first (Lionello et al., 2006).

In the north-western Mediterranean Sea, the Northern Current (NC) represents the main feature of the surface circulation transporting waters alongshore from the Ligurian Sea to the Alboran Sea (Fig. 1a). North-east of the Balearic Promontory a surface oceanographic front separates Mediterranean waters transported by the NC from the Atlantic waters that recently entered the Mediterranean (Millot, 1999; Pinot et al., 2002; André et al., 2005).

Deep convection occurs offshore the GoL due to the action of very intense cold and dry winter winds such as the Tramontana and the Mistral. These winds cause strong evaporation and cooling of surface water thus increasing their density until sinking to greater depths leading to Western Mediterranean Deep Water (WMDW) (MEDOC, 1970; Lacombe et al., 1985; Millot, 1999). Dense shelf water cascading (DSWC) in the GoL also contributes to the sink of large volumes of water and sediments into the deep basin (Canals et al., 2006).

The north-western Mediterranean is subject to an intense bloom in late winter-spring when the surface layer stabilizes, and sometimes to a less intense bloom in autumn, when the strong summer thermocline is progressively eroded (Estrada et al., 1985; Bosc et al., 2004; D'Ortenzio and Ribera, 2009; Siokou-Frangou et al., 2010). SST in the region evolve accordingly with this bloom seasonality, with minima SST in February, which subsequently increases until maxima summer values during August. Afterwards, a SST drop can be observed on October although with some interanual variability (Pastor, 2012).

3 Material and methods

3.1 Sediment cores description

The studied sediment cores were recovered from a sediment drift built by the action of the southward branch of the WMDW north of Minorca (Fig. 1). Previous studies carried out at this site already described high sedimentation rates (> 20 cm kyr^{-1}) (Frigola et al., 2007, 2008; Moreno et al., 2012), which initially suggested a suitable location to carry on a detailed study of the last millennia. The cores were recovered from two different stations at about 50 km north of Minorca Island with a multicore system. Cores MINMC06-1 and MINMC06-2 (henceforth MIN1 and MIN2) (40°29'N, 04°01'E; 2391m water depth; 31 and 32.5 cm core length, respectively) were retrieved in 2006 during HERMES 3 cruise onboard the R/V Thethys II. In reference to the recovery of cores HER-MC-MR3.1, HER-MC-MR3.2 and HER-MC-MR3.3 (henceforth MR3.1, MR3.2 and MR3.3) (40°29'N, 3°37'E; 2117m water depth; 27, 18 and 27 cm core length, respectively) took place in 2009 during HERMESIONE expedition onboard the R/V Hespérides. The distance between the MIN and the MR3 cores is ~30 km and both stations are located in an intermediate position within the sediment drift, which extends along a water depth range from 2000 to 2700m (Frigola, 2012; Velasco et al., 1996; Mauffret et al., 1979), being MIN cores deeper than the MR3 ones by about ~300m.

MIN cores were homogeneously sampled at 0.5 cm resolution in the laboratory while for MR3 cores a different strategy was followed. MR3.1 and MR3.2 were initially subsampled with a PVC tube and splitted in two halves for XRF analyses in the laboratory. Both halves of core MR3.1, MR3.1A and MR3.1B, were used for the present work as replicates of the same core and records for each half are shown separately. All MR3 cores were sampled at 0.5 cm resolution for the upper 15 cm and at 1 cm for the rest of the core, with the exception of half MR3.1B that was sampled at 0.25 cm resolution. MR3 cores were formed by brown-orange nanofossil and foraminifera silty clay, lightly bioturbated, with the presence of enriched layers in pteropods and gastropods fragments and some dark layers.

Additionally, core top samples from seven multicores collected at different locations in the western Mediterranean have also been used for the correction of the Mg/Ca-SST calibration from *G. bulloides* (Table 1; Fig. 1).

3.2 Radiocarbon analyses

Twelve ^{14}C AMS dates were performed on cores MIN1, MIN2 and MR3.3 (Table 2) over 4–22mg samples of planktonic foraminifer *Globigerina inflata* handpicked from the > 355 μm fraction. Ages were calibrated with the standard marine correction of 408 years and the regional average marine reservoir correction (ΔR) for the central-western Mediterranean Sea using Calib 7.0 software (Stuiver and Reimer, 1993) and the MARINE13 calibration curve (Reimer et al., 2013).

3.3 Radionuclides ^{210}Pb and ^{137}Cs

The concentrations of the naturally occurring radionuclide ^{210}Pb were determined in cores MIN1, MIN2, MR3.1A and MR3.2 by alpha-spectroscopy following Sanchez-Cabeza et al. (1998). Concentrations of the anthropogenic radionuclide ^{137}Cs in core MIN1 were measured by gamma spectrometry using a high purity intrinsic germanium detector. Gamma measurements were also used to determine the ^{226}Ra concentrations via the gamma emissions of ^{214}Pb, used to calculate the excess ^{210}Pb concentrations. Sediment accumulation rates for the last century were calculated using the CIC (constant initial concentration) and the CF : CS (constant flux : constant sedimentation) models (Appleby and Oldfield, 1992; Krishnaswami et al., 1971), constrained by the ^{137}Cs concentration profile for core MIN1 (Masqué et al., 2003).

3.4 Bulk geochemical analyses

The elemental composition of cores MR3.1B and MR3.2 was obtained with a XRF Core-Scanner Avaatech System (CORELAB, University of Barcelona), which is equipped with an optical variable system that allows determining in an independent way the length (10–0.1mm) and the extent (15–2 mm) of the bundle of beams-X. This allows obtaining qualitative information of the elementary composition of the materials. The core surfaces were scraped cleaned and covered with a 4 μm thin SPEXCertiPrep Ultralene foil to prevent contamination and minimize desiccation (Richter and van der Gaast, 2006). Sampling was performed every 1 cm and scanning took place directly at the split core surface. Among the several measured elements this study has mainly use the Mn profile in the construction of the age models.

3.5 Planktonic foraminifera analyses

Specimens for the planktonic foraminifera *Globigerina bulloides* for Mg/Ca and $\delta^{18}O$ measurements were picked together from a very restrictive size range (250-355 microns) but then crushed and cleaned separately. In core MR3.1B, picking was often performed in the <355 μm fraction due to the small amount of material (sampling every 0.25 cm). Additionally, quantitative analysis of planktonic foraminifera assemblages was carried out in core MR3.3 and on the upper part of core MR3.1A by using the fraction size above 125 μm. The 42 studied samples presented abundant and well-preserved planktonic foraminifera.

Samples for trace elements analyses were formed by ~45 specimens of *G. bulloides*, crushed under glass slides to open the chambers and carefully cleaned applying a sequence of clay removal, oxidative and weak acid cleaning steps (Pena et al., 2005). Only samples from core MR3.1A were cleaned including also the "reductive step". Instrumental analyses were performed in an inductively coupled plasma mass spectrometer (ICP-MS) Perkin Elmer in the Scientific and Technological Centers of the University of Barcelona (CCiT-UB). A standard solution with a ratio close to the foraminifera values (3.2 mmol mol^{-1}) was run every four samples in order to correct any drift over the measurement runs for MR3.1 halves. Standard solution used on the rest of analyses was low (1.6 mmol mol^{-1}). The average reproducibility of Mg/Ca ratios, taking into account the known standard solutions concentrations, was 97 and 89% for MIN1 and MIN2 cores, and 99 and 97% for MR3.1A, MR3.1B and MR3.3 cores, respectively Procedure blanks were also routinely measured in order to detect any potential contamination problem during the cleaning and dissolution procedure. Mn/Ca and Al/Ca ratios were always measured in order to detect any potential contamination problem associated with the presence of Mn oxydes and aluminosilicates (Barker et al., 2003; Lea et al., 2005; Pena et al., 2005).

In order to avoid the overestimation of Mg/Ca-SST by detrital contamination, Mn/Ca values > 0.5 mmol mol^{-1} were discarded in core MR3.1B and only those higher than 1 mmol mol^{-1} on MIN1 and MR3.3. With regard to Al/Ca data, those values susceptible of contamination were also removed. After this data cleaning any significant statistical correlation existed between Mg/Ca and Mn/Ca; Al/Ca (r has been always lower than 0.29, p-value=0.06).

Mg/Ca ratios were transferred into SST values using the calibration proposed in this study (Section 5.1). In the case of the record MR3.1A, cleaned with the reductive procedure, the Mg/Ca ratios were about 23% lower than those measured in core MR3.1B without the reductive step. This ratio lowering is expected from the preferential dissolution of the Mg-enriched calcite during the reductive step (Barker et al., 2003; Pena et al., 2005; Yu et al., 2007). The obtained percentage of Mg/Ca lowering is comparable or higher to those previously estimated for different planktonic foraminifera, although data from *G. bulloides* was not previously reported (Barker et al., 2003). SST-Mg/Ca in core MR3.1A was calculated after the Mg/Ca correction of this 23% offset and applying the same calibration than with the other records.

Stable isotopes measurements were performed on 10 specimens of *G. bulloides* after sonically cleaned in methanol to remove fine-grained particles. Analyses were performed in a Finnigan-MAT 252 mass spectrometer fitted with a carbonate microsampler Kiel-I in the CCiT-UB. Analytical precision of laboratory standards for $\delta^{18}O$ is better than 0.08 ‰. Calibration to Vienna Pee Dee Belemnite or V-PDB was carried out by means NBS-19 standards (Coplen, 1996).

Seawater $\delta^{18}O$ ($\delta^{18}O_{SW}$) was obtained after removing the temperature effect on the *G. bulloides* $\delta^{18}O$ record by applying the Mg/Ca-SST records in the Shackleton Paleotemperature Equation (Shackleton, 1974). The results are expressed in the water standard SMOW ($\delta^{18}O_{SW}$) after the correction of Craig (1965). It was also considered the use of specific temperature equations for *G. bulloides* (Bemis et al., 1998; Mulitza et al., 2003), but the core tops estimates provided $\delta^{18}O_{sw}$ values of 2.2-1.8 ‰, significantly higher than those (~1.2 ‰) measured in water samples from the central-western Mediterranean Sea (Pierre, 1999). Considering that the core top $\delta^{18}O_{sw}$ estimates, after the application of the empirical Shackleton (1974) paleotemperature equation, averaged 1.3 ‰ and thus closer to the actual water measurements, it was decided that this equation was providing more realistic oceanographical conditions in this location.

3.6 Alkenones

Measurements of the relative proportion of unsaturated C_{37} alkenones, namely $U^{k'}_{37}$ index, were carried out in order to obtain SST records on the studied cores. Detailed information about the methodology and equipment used in C_{37} alkenone determination can be found in Villanueva et al. (1997). The precision of this paleothermometry tool has been determined as close as ± 0.5°C (Eglinton et al., 2001). Furthermore, taking into account duplicate alkenone analysis carried out in core MR3.3, the precision achieved results better than ± 0.8°C. Reconstruction of SST records was based on the global calibration of Conte et al. (2006).

4 Age model development

Obtaining accurate chronologies for each of the studied sediment cores is particularly critical to allow their direct comparison and produce a stack record that represents the regional climatic signal. With this objective, a wide set of parameters have been combined in order to obtain chronological markers in all the studied sedimentary records, including absolute dates and stratigraphical markers based on both geochemical and micro-paleontological data (Table 3; Table S.1).

4.1 ^{14}C, ^{210}Pb, ^{137}Cs dates

Absolute dating with radiocarbon dates was focused on cores MIN1, MIN2 and MR3.3 (Table 2). According to those dates and assuming the sampling year as the core top age (2006 and 2009, respectively), the sedimentation rates of these three cores result in 13 ± 1, 20 ± 3 and 13 ± 5 cm ky^{-1}, respectively (uncertainties are expressed as 1 σ).

In order to evaluate the preservation of the core tops, ^{210}Pb activity profiles were obtained from cores MIN1, MIN2, MR3.1A and MR3.2 (Fig. 2). ^{210}Pb concentrations generally decrease with depth in all four cores, down to 3.5 cm in core MIN2 and 3 cm for cores MIN1, MR3.1A and MR3.2. Excess ^{210}Pb concentrations at the surface and inventories in the MIN cores are in agreement with those published for the Algero-Balear Basin (Garcia-Orellana et al., 2009). However, they were lower in MR3 cores, particularly for core MR3.1A, which we attribute to the loss of the most surficial part of these cores during recovery, corresponding to about 50 yr by comparison to the other cores. The variability in the ^{210}Pb data denotes the high heterogeneity of this sedimentary system in reference to deep-sea hemipelagic sediments, highlighting the relevance of its study on the basis of a multicore approach (e.g. Maldonado et al., 1985; Martin et al., 1989; Calafat et al., 1996; Velasco et al., 1996; Canals et al., 2006; Frigola et al., 2007).

The concentration profile and inventory of ^{137}Cs in core MIN1 is also in good agreement with the results reported for the Western Mediterranean Basin (Garcia-Orellana et al., 2009). Its detection down to 3 cm combined with the excess ^{210}Pb concentration profile suggests the presence of sediment mixing to be accounted for in the calculation of the sediment accumulation rates, which are to be taken as maxima estimates. In doing so, the maxima sedimentation rates for the last 100–150 years are (uncertainties are expressed as 1 σ): 27 ± 2 cm kyr^{-1} (core MIN1), 28 ± 2 cm kyr^{-1} (MIN2), 28 ± 4 cm kyr^{-1} (MR3.1A), and 35 ± 3 cm kyr^{-1} (MR3.2). These sedimentation rates are in agreement with those previously described in a long sediment record recovered within the contouritic system (Frigola et al., 2007 and 2008), but much higher than those found in the literature from deeper sites of the Balearic Sea, with predominant hemipelagic sedimentation (e.g. Weldeab et al., 2003; Zúñiga et al., 2007; Garcia-Orellana et al., 2009).

4.2 Biostratigraphical data based on planktonic foraminifera

Core MR3.3, the best ^{14}C-dates time-constrained, was chosen in order to perform a taxonomic analysis of planktonic foraminifera. The identified species were: (1) *Globigerina bulloides* including *G. falconensis*, (2) *Globigerinoides ruber* pink and white variety, (3) *Orbulina* spp. including both *O. universa* and *O. suturalis*, (4) *Globigerinoides quadrilobatus* and *G. sacculifer*, (5) *Globigerinatella siphoniphera* including *G. calida*, (6) *Globorotalia inflata*, (7) *Turborotalita quinqueloba*, (8) *Globigerinita glutinata*, (9) *Neogloboquadrina pachyderma* right coiled, (10) *Neogloboquadrina dutertrei*, (11) *Globorotalia truncatulinoides* left coiled and (12) *Clavoratorella* spp. The abundance of *G. truncatulinoides* left coiled was also analysed in the top of the core MR3.1A.

In order to improve the time constrain of our cores, percentages records of *G.*

quadrilobatus and *G. truncatulinoides* left coiled from core MR3.3 have been correlated with those from a southern Tyrrhenian Sea composite core (Fig. 3), with a very robust age-model (Lirer et al., 2013) based on the combination of different dating methods (radionuclides-^{14}C AMS dates and tephra-chronology). The Mediterranean eco-biostratigraphic strength of the distribution patterns of these taxa has been previously documented by Piva et al. (2008) for the last 370ky. The pronounced decrease in *G. quadrilobatus* percentages at the base of core MR3.3 (Fig. 3a) can be correlated with the end of the *G. quadrilobatus* acme interval observed in the north and south Tyrrhenian Sea record (Lirer et al., 2013, 2014; Di Bella et al., 2014) from 1750 to 750 yr BCE and previously documented in the Sicily Channel (Sprovieri et al., 2003) and the Sardinian valley (Budillon et al., 2009). In addition, data on distribution pattern of the leaving planktonic foraminifera, reported in Pujol and Vergnaud-Grazzini (1995), documented that this taxon is present in the whole central and south western Mediterranean (excluding the GoL). This correlation provide to us a control age point in core MR3.3 of 750 ± 48 BCE at about 27 cm, consistent with the ^{14}C dating of 301 ± 87 yr BCE at 24 cm. In the upper part of the MR3.3 record, another control age point can be obtained from the correlation of the pronounced peak of *G. truncatulinoides* left coiled (~20% in abundance, Fig. 3b) with a similar peak previously reported in the central and south Tyrrhenian Sea record during the LIA at 1718 ± 10 yr CE (Lirer et al., 2013; Margaritelli et al., 2015), and coincident with the Maunder event (Vallefuoco et al., 2012; Lirer et al., 2014; Margaritelli et al., 2015). Thunell (1978) documented the occurrence in recent surface sediments of this taxon from Balearic Islands to Sicily channel and Pujol and Vergnaud-Grazzini (1995) observed this species in leaving abundance foraminifera of the whole western Mediterranean. This age point is also consistent with the obtained ^{14}C date of core MR3.3 at 3.5cm of 1434 ± 51 yr CE, further supporting the absence of the last two centuries in the core MR3.3. The absence of these centuries is also suggested by the *G. truncatulinoides* left coiled abundance patterns data from the top (1.5–3.5 cm) of the core MR3.1A (Fig. 3b). MR3.1A data is in agreement with the drop of the peak in core MR3.3 and ^{210}Pb measurements (Fig. 2) have corroborated the presence of the most recent sediment in core MR3.1A.

4.3 Bayesian accumulation models

A preliminary age model for cores MIN1, MIN2 and MR3.3 was initially generated by means of available ^{14}C ages, the two biostratigraphical dates from core MR3.3 and maximum sedimentation rates derived from ^{210}Pb concentration profiles from cores MIN1 and MIN2. This preliminary age model was built using the Bayesian statistics software Bacon with the statistical package R (Blaauw and Christen, 2011).

Considering that the two independent sedimentation rates estimations based on ^{14}C and ^{210}Pb have significant uncertainties inherent to the methods and considering the different sampling resolution, averaged sedimentation rates obtained from the two methods have been taken into account in the Bayesian accumulation models. Regarding the core top ages, it was considered to be the recovering year (2006 ± 10 yr CE) in MIN cores and 1718 ± 10 yr CE for core MR3.3, coinciding with the peak in the *G. truncatulinoides* record. The program settings for thickness of the sections and memory were chosen to fulfil the criterions of the best mean 95% confidence range and to maintain good correlation between prior and posterior accumulation rates. In addition, it was decided to keep the memory strength values rather high since the sedimentary context, a contouritic drift, is expected to record highly variable accumulation rates, and due to the smother changes induced by lowering the memory strength would no reflect realistic changes in this context.

The best Bayesian models achieved with a confidence mean of 95% provide accumulation rates for cores MIN1, MIN2 and MR3.3 of 14 ± 2, 22 ± 1 and 12 ± 1 cm kyr^{-1}, respectively (uncertainties are expressed as 1 σ), which correspond to mean time resolutions of 292, 161, and 200 yr, respectively. It should be noted that the largest errors are obtained for core MIN1 because of the only two ^{14}C dates. These age models reconstruct a rather smooth accumulation history, although significant fluctuations in accumulation rate at centennial or even decadal scale can be expected in this sedimentological context. The posterior outputs for accumulation rate (see Fig. 4) and its variability are quite comparable to their prior ones, but in the case of core MR3.3 the posterior output indicates larger memory (more variability) than that assumed a priori. This is due to the strong change in sedimentation rates at about 12 cm (998 yr CE) that the prior output tends to attenuate, and which could be associated with abrupt changes in sedimentation rates at that time (Fig. 4c).

These age models have been then further re-evaluated using other geochemical proxies as stratigraphical tools in order to ensure a common chronological framework for the obtained climate records (Sect. 4.4). Nevertheless, any readjustment has always been kept within the confident rage of the Bayesian models.

4.4 Multi-proxy chronostratigraphy

The chronologies of cores MIN1, MIN2 and MR3.3 were finally evaluated and readjusted in base to their Mg/Ca records and taking into account the 95% probability intervals obtained in the Bayesian models.

Mg/Ca measured in *G. bulloides* is a well-established proxy of Sea Surface Temperatures (Barker et al., 2005). The two sampling stations are only separated by 30 km and thus it is a reasonable assumption to expect comparable and synchronous SST changes in all the studied cores. Visual comparison of the MIN1, MIN2 and MR3.3 records of Mg/Ca show several resemblances in some of the main patterns and structures, which are considerably synchronous with the Bayesian age models (Fig. 5). Consequently, the three records have been tuned in base to the main structures and taking into account the 95% confidence of the statistical produced models (Fig. 5). The final age-models of cores MIN1, MIN2 and MR3.3 have an average age difference that is below 24 years in reference to the Bayesian models and the 75–63% of the records are into the confidence intervals obtained in the Bayesian models.

The chronology from core MR3.3 has been the base to construct the age model for the other MR3 cores (MR3.1A, MR3.1B and MR3.2) for which no ^{14}C dates were available (Table 3). The chronostratigraphical tools for core MR3.1 have been again the Mg/Ca records (Fig. 5; Supplementary Information, Table S1). Additionally, manganese records in all MR3 cores have also been used as an additional chronostratigraphical tool. Mn presence in deep-sea sediments is related to redox processes (Calvert and Pedersen, 1996). Considering that all MR3 cores correspond to the same multicore these Mn rich layers have been used as isochrones. The available Mn records have been measured by two different methods: Mn measured in the bulk sediment by means of XRF Core-Scanner (MR3.1B and MR3.2) and Mn present in the foraminifera samples and measured by ICP-MS (MR3.3, MR3.1A and MR3.1B). Absolute values were very different between those samples measured with ICP-MS after cleaning the foraminifera with the reductive step (MR3.1A) and those without this cleaning step (MR3.3 and MR3.1B) but the same main features can be correlated between the three cores (Fig. 6; Supplementary Information, Table S1). In the case of core MR3.1B (Fig. 6b), analysed at ultra-high resolution (0.25 cm slides), the Mn record shows the highest values with peaks over 80 ppb whose Mg/Ca values have been excluded of derived SST records since Mn enrichments can bias Mg/Ca ratios toward higher values and lead to significant overestimation of past seawater temperatures

(Boyle, 1983; Pena et al., 2005, 2008). The top 5 cm of cores MR3.1A and MR3.2 have been dated according to the maxima sedimentation rates using the ^{210}Pb flux.

4.5 Final age models and associated sedimentation rates

According to the obtained chronologies, the period covered by the studied sedimentary sequences is from 759 ± 20 yr BCE to 1988 ± 18 yr CE (uncertainties are expressed as the time resolution of the respective core here and in 1σ on the rest of the section), being core MR3.1B the one spanning a longer period (Table 4). Total average of mean accumulation rates is 17 ± 4 cm ky^{-1} with a total mean resolution of 84 ± 18 years.

The final mean sedimentation rates obtained in MIN cores, 14 ± 6 and 25 ± 10 cm kyr^{-1}, are very similar with those derivated from Bayesian model simulations, 14 ± 2 and 22 ± 1 cm kyr^{-1}, and those previously published by Moreno et al. (2012), 19 and 23 cm kyr^{-1}.

The differences in sedimentation rates between all cores except MIN2 are lower than 3 cm kyr^{-1}, variability that is reasonable due the diverse sediment processes that affect the contouritic system.

5 Sea surface temperatures and $\delta^{18}O$ data

5.1 Mg/Ca-SST calibration

The Mg/Ca ratio measured in *G. bulloides* is a widely used proxy to reconstruct SST (Barker et al., 2005) although available calibrations can provide very different results (Lea et al., 1999; Mashiotta et al., 1999; Elderfield and Ganssen, 2000; Anand et al., 2003; McConnell and Thunell, 2005; Cléroux et al., 2008; Thornalley et al., 2009; Patton et al., 2011). Apparently, the regional Mg/Ca-temperature response varies due to parameters that have not yet been identified (Patton et al., 2011). A further difficulty arises from the questioned Mg/Ca-thermal signal in high salinity regions such as the Mediterranean Sea where anomalous high Mg/Ca values have been observed (Ferguson et al., 2008). This apparent high salinity sensitivity in foraminifera-Mg/Ca ratios is under discussion and it has not been supported by recent culture experiments (Hönisch et al., 2013), which in addition, could be attributed to diagenetic overprints (Hoogakker et al., 2009; van Raden et al., 2011). In order to test the value of the Mg/Ca ratios in *G. bulloides* from the western Mediterranean Sea and also review its significance in terms of seasonality and depth habitat, a set of core top samples from different locations of the western Mediterranean Sea have been analysed. Core-top samples were recovered using a multicorer system and they can be considered as representative of near or present conditions (Masqué et al., 2003; Cacho et al., 2006). The studied cores are included in the 35–45° N latitude range (Table 1 and Fig. 1) and mostly represent two different trophic regimes, defined by the classical spring bloom (the most north-western basin) and an intermittently bloom (D'Ortenzio and Ribera, 2009).

The obtained Mg/Ca ratios have been compared with the isotopically derived calcification temperatures based on the $\delta^{18}O$ measurements performed also in *G. bulloides* from the same samples. This estimation was performed after applying the Shackleton (1974) paleotemperature equation and using the $\delta^{18}O_{water}$ data published by Pierre (1999), taking always into consideration the values of the closer stations and from the top 100 m. The resulting Mg/Ca-SST data have been plotted together with those *G. bulloides* data points from North Atlantic core tops previously published by Elderfield and Ganssen (2000). The resulting high correlation ($r^2 = 0.9$; Fig. 7a) strongly supports the dominant thermal signal in the Mg/Ca ratios of the central-western Mediterranean Sea. Thus, the new data set from the Mediterranean core tops improves the sample coverage over the warm end of the calibration and the resulting exponential function indicates 9.7 % sensitivity in the Mg uptake respect to temperature, which is in agreement with the described range in the literature (i.e., Elderfield and Ganssen, 2000; Barker et al., 2005; Patton et al., 2011). The new calibration obtained from the combination of Mg/Ca-SST data from the western Mediterranean Sea and Atlantic Ocean is:

$$Mg\ /\ Ca = 0.6788(\pm 0.1011)e^{0.0973(\pm 0.0097)T} \qquad (1)$$

The Mg/Ca-SST signal of *G. bulloides* has been compared with a compilation of water temperature profiles of the first 100 m measured between 1945–2000 yr in stations close to the studied core tops (MEDAR GROUP, 2002). Although significant regional and interannual variations have been observed, the obtained calcification temperatures of our core top samples present the best agreement with temperature values of the upper 40 m during the spring months (April–May) (Fig. 7b). This water depth is consistent with that found by plankton tows in the Mediterranean (Pujol and Vergnaud-Grazzini, 1995) and with results from multiannual sediment traps monitoring in the Alboran Sea and the GoL where maximum percentages were observed just before the beginning of thermal stratifications (see Bárcena et al., 2004; Bosc et al., 2004; Rigual-Hernández et al., 2012). Although the available information about depth and seasonality distribution of *G. bulloides* is relatively fragmented, this species is generally situated in intermediate or even shallow waters (i.e. Bé, 1977; Ganssen and Kroon, 2000; Schiebel et al., 2002; Rogerson et al., 2004; Thornalley et al., 2009). However, *G. bulloides* has been also observed at deeper depths in some western Mediterranean Sea sub basins (Pujol and Vergnaud-Grazzini, 1995). Extended data with enhanced spatial and seasonal coverage are required in order to better characterise production, seasonality, geographic and distribution patterns of live foraminifers as *G.bulloides*. Nevertheless, the obtained core top data set offers a solid evidence about the seasonal character of the recorded temperature signal in the Mg/Ca ratio.

5.2 A regional stack for SST-Mg/Ca records

The obtained Mg/Ca-SST profiles obtained from our sediment records are plotted with the resulting common age model in Fig. 8. The average SST values for the last 2700 years are 18.0 ± 0.8°C (attendant uncertainties of average values are given in 1**σ in this section**). All the temperature reconstructions show the warmest sustained period during the RP, approximately between 170 yr BCE to 300 yr CE, except core MIN2, since this record ends at the RP-DA transition. In addition, all the records show a general consistent cooling trend after the RP with several centennial scale oscillations. Maximum Mg/Ca-SST value is observed in core MR3.3 (21.0 ± 0.7°C) during the RP (Fig. 8c) and the minimum is recorded in core MIN1 (15.3 ± 0.9°C) during the LIA (Fig. 8e). The records present high centennial-scale variability. Particularly, during MCA some warm events reached SST comparable to those of the RP and lightly higher than the average of maxima SST (20.3 ± 0.6°C), but they were far shorter in duration (Fig. 8). The highest frequency of intense cold events occurred during the LIA and, especially, the last millennia recorded the minima average Mg/Ca-SST (16.1 ± 0.8°C). Four of the five records show a pronounced minima SST after year 1275 CE when occurred the onset of LIA. In base to the differentiated patterns in Mg/Ca-SST the LIA period has been divided into two subperiods, an early warmer interval (LIAa) and a later colder interval (LIAb) with the boundary located at 1540 yr CE.

One of the main difficulties of working with SST reconstructions for the last millennia is that the targeted climatic signal has often a comparable amplitude to the internal noise of the records due to sampling and proxy limitations. In order to minimize this inherent random noise, all the studied records have been combined in a regional

Mg/Ca-SST anomaly stack with the aim to detect the most robust climatic structures along the different records and reduce the individual noise. Firstly, each SST record was converted into a SST anomaly record in relation to its average temperature (Fig. 8f). Secondly, in order to obtain a common sampling interval all records were interpolated. Although interpolation was performed at 3 different resolutions, results did not differ substantially (Fig. 8g). Subsequently, we selected the stack that provided the best resolution offered by our age models (20 yr cm^{-1}) since it preserves very well the high frequency variability of the individual records (Fig. 8g).

The obtained stack represents in a clearer way the main SST features described earlier and allows to better identifying the most significant features at centennial-time scale. The most abrupt cooling events are recorded during the LIA (-1 ± 0.4 °C in 100 yr) while the most abrupt warming (0.9 ± 0.4°C in 100 yr) is detected during the beginning of MCA. When the whole studied period is considered a long term cooling trend of about -0.5°C is observed; however if we focus on the last 1800 yr, since the RP maxima, the observed cooling trend was far more intense, of about -2.4°C. The long term cooling trend is in good agreement with the recent 2k global reconstruction published by McGregor et al., (2015) (best estimation of the SST cooling trend, using the average anomaly method 1 for the periods 1-2000 CE: -0.3°C/kyr to -0.4°C/kyr). Although, the cooling trend of the last 1800 yr observed in our data (~1.3 ± 0.4°C/kyr) is larger than those estimated in the global reconstruction for the last 1200 yr (average anomaly method 1: -0.4°C/kyr to -0.5°C/kyr), It should be noted that this study includes Alk-SST from MIN cores (data published in Moreno et al., 2012)

5.3 Oxygen isotope records

Oxygen isotopes measured on carbonates shells of *G. bulloides* ($\delta^{18}O_c$) and their derived $\delta^{18}O_{SW}$ after removing the temperature effect with Mg/Ca-SST records (see Sect. 3.5) are shown in Fig. 9. $\delta^{18}O_c$ and their derived $\delta^{18}O_{SW}$ profiles have been respectively stacked following the same procedure for the SST-Mg/Ca stack (see Sect. 5.2). In general terms, all the records present a high stable pattern during the whole period with a weak depleting trend, which is almost undetectable in some cases (i.e. core MIN1).

Average $\delta^{18}O_c$ values are 1.3 ± 0.1 VPDB‰ (uncertainty are expressed with a 1σ in this section) and, in general, MR3 cores show lightly heavier values (1.4 VPDB‰) than MIN cores (1.2 VPDB‰). Lightest $\delta^{18}O_c$ values (1.1 ± 0.1 VPDB‰) mostly occur during the RP, although some short light excursions can be also observed during the end of the MCA and/or the LIA. Heaviest values (1.6 ± 0.2 VPDB‰) are mainly associated with short events during the LIA, the MCA and over the TP/RP transition. A significant increase of $\delta^{18}O_c$ values is observed at the LIA/IE transition, although a sudden drop is recorded at the end of the stack record (after 1867 yr CE), which could result from a differential influence of the records (i.e. MIN1) and/or extreme artefact (Fig. 9g).

After removing the temperature effect on the $\delta^{18}O_c$ record, the remaining $\delta^{18}O_{SW}$ record mainly reflects changes in E–P balance, thus resulting as an indirect proxy for sea surface salinity. The average $\delta^{18}O_{SW}$ values obtained for the studied period are 1.8 ±0.2 SMOW‰. Heaviest $\delta^{18}O_{SW}$ values (2.2 ± 0.2 SMOW‰) are recorded during the RP when the longest warm period is also observed. Enhancements of the E–P balance ($\delta^{18}O_{SW}$ heavier values) are coincident with higher SST (Fig. 11). Lightest $\delta^{18}O_{SW}$ values (1.3 ± 0.3 SMOW‰) are recorded particularly during the onset and the end of the LIA and also during the MCA. A drop in the E–P balance has been obtained approximately from the end of LIA to the most recent years. The $\delta^{18}O_{SW}$ stacked record show variations during the studied period ranged about ± 0.2 20 yr^{-1} (~0.8 PSU 20 yr^{-1}; Fig. 9). The most significant changes in our $\delta^{18}O_{SW}$ (salinity) stack record correspond to an increase around 1000 yr CE and the decrease observed at the end of the LIA.

5.4 Alkenone-SST records

The two alkenone ($U^{k'}_{37}$)-derived SSTs of MIN cores were already published in Moreno et al. (2012), while the records from MR3 cores are new (Fig. 10). The four Alkenone-SST records show a similar general cooling trend during the studied period and they have also been integrated in a SST anomaly stack (Fig. 10e). The whole cooling trend is of about -1.6°C when the whole studied period is considered and about -2°C since the SST maximum recorded during the RP. Previous studies have interpreted the Alkenone-SST signal in the western Mediterranean Sea as an annual average (Ternois et al., 1996; Cacho et al., 1999a, b; Martrat et al., 2004). The average Alkenone-SST for the studied period (last 2700 yr) is 17.2 ± 0.2°C (uncertainty in average values is expressed with a 1 σ), which is in substantial agreement with the annual mean corresponding to a Balearic site (18.7 ± 1.1°C) according to the integrate values of the upper 50 m (Ternois et al., 1996; Cacho et al., 1999a) of the GCC-IEO database that covers January 1994–July 2008.

The alkenone temperatures ranged between 16.0 ± 0.8°C, core MIN2 during the LIAa, and 18.4 ± 0.8°C, core MR3.3 during the MCA). Values near the average of maxima SST (18.1 ± 0.2°C) are observed more frequently during TP, RP and MCA, while temperatures during the onset of MCA and LIA show many values closer to the average of minima SST (16.2 ± 0.1°C). The most abrupt coolings (-0.3°C 20 yr^{-1}) are observed at the end of the XX century (-0.8°C 100 yr^{-1}) and the end of the MCA, while the highest warming rates (+0.3°C 20 yr^{-1}; +0.5°C 100 yr^{-1}) are recorded during the MCA.

5.5 Mg/Ca vs. Alkenone SST records

The mean Alkenone-SST values are about 1°C colder than those from the Mg/Ca- SST reconstruction: 17.2 ± 0.2 vs. 18.0 ± 0.8°C (SST-uncertainties in this section are expressed as 1σ). This difference cannot be attributed to the different habitat depth since alkenones should reflect the surface photic layer (<50 m), while *G. bulloides* has the capability to develop in a wider and deeper environment (Bé, 1977; Pujol and Vergnaud-Grazzini, 1995; Ternois et al., 1996; Sicre et al., 1999; Ganssen and Kroon, 2000; Schiebel et al., 2002; Rogerson et al., 2004; Thornalley et al., 2009). Consequently this proxy difference should be associated with the growing season of the signal carriers. $U^{k'}_{37}$-SST records in the western Mediterranean Sea have been interpreted to represent mean annual SST (i.e. Cacho et al., 1999a; Martrat et al., 2004) but seasonal variations in alkenone production could play an important role in the $U^{k'}_{37}$-SST values (Rodrigo-Gámiz et al., 2014). Considering that during the summer months the Mediterranean Sea is a very stratified and oligotrophic sea, it should be expected reduced alkenone production during this season (Ternois et al., 1996; Sicre et al., 1999; Bárcena et al., 2004; Versteegh et al., 2007; Hernández-Almeida et al., 2011). This observation is further supported by the results from sediment traps located in the GoL showing very low coccolith fluxes during the summer months (Rigual-Hernández et al., 2013), while they show higher values during autumn, winter and spring, reaching maximum values at the end of the winter season, during SST minima. In contrast, high fluxes of *G. bulloides* are almost restricted to the upwelling spring signal, when coccolith fluxes have already started to decrease (Rigual-Hernández et al., 2012, 2013). This different growth season can explain the proxy bias in the SST reconstructions, with colder SST recorded by the alkenones.

Both Mg/Ca-SST and $U^{k'}_{37}$-SST records show a consistent cooling trend during the studied period, which since the RP maxima is of about 2°C in the alkenones record and 2.4°C in the Mg/Ca record. This last cooling is larger than those estimated in the global reconstruction (McGregor et al., 2015) for the last 1200 yr (average anomaly method 1: -0.4°C/kyr to -0.5°C/kyr). Instead, differences with the cooling observed in our alkenone records are lower. It should be note that the global reconstruction includes Alk-SST from MIN cores (data published in Moreno et al., 2012).

The enhanced Mg/Ca-SST variability is also reflected in the short term oscillations, at centennial time scale, which are better represented in the Mg/Ca record with oscillations over 1°C, while in the alkenone record are mostly shorter than 0.5°C. This enhanced Mg/Ca-SST variability could be also attributed to the highly restricted seasonal character of its signal, which purely reflects SST changes during the spring season. However, the coccolith signal integrates a wider time period from autumn to spring (Rigual-Hernández et al., 2012, 2013) and, consequently, changes associated with specific seasons become more diluted in the resultant averaged signal.

The detailed comparison of the centennial SST variability recorded by both proxy stacks consistently indicates a puzzling antiphase (Fig. 11b and c). Although the main trends are consistently parallel in both alkenone and Mg/Ca proxies ($r=0.5$; p value=0) as has been noted in other regions, short-term variability appears to have an opposite character. Results obtained by means of Welch's test indicate that the null hypothesis (means are equal) can be discarded at he 5% error level: $t_{observed}$ (12.446)>$t_{critical}$ (1.971). This unexpected outcome is a firm evidence of the relevance of the seasonal variability in the climate evolution and would indicate that extreme winter coolings were followed by a more rapid and intense spring warmings. Nevertheless, regarding the low amplitude of several of these oscillations, often close to the error of the proxies, this observation needs to probed with further constrains as a solid regional feature.

6 Discussion

6.1 Climate patterns during the last 2.7 kyr

Changes in SST in the Minorca region have implications in the surface air mass temperature and moisture source regions that would determine air mass trajectories and ultimately precipitation regime in the Western Mediterranean Region (Millán et al., 2005; Labuhn et al., 2015). Observations of recent data have identified SST as a key factor in the development of torrential rain events in the Western Mediterranean Basin (Pastor et al., 2001), being able to act as a source of potential instability of air masses that transit over these waters (Pastor, 2012). In this line, the combination of SST reconstruction with δ^{18}Osw can provide a light to analyse the connection between thermal changes and moisture export from the central-western Mediterranean Sea during the last 2.7 kyr.

The older period recorded by our records is the so-call Talaiotic Period (TP), which corresponds to the Ancient Ages as the Greek Period in other geographic areas. Both studied SST proxies are consistent showing a general cooling trend from ~500 yr BCE and reaching minimum values by the end of the period (~120 yr BCE), synchronously with a reduction in the E–P rate occurred (Fig. 11a–c). Very few other records exist from this time period to compare these trends at regional scale.

One of the most outstanding features in the two SST-reconstructions, particularly in the Mg/Ca-SST stack is the warm SST that dominated especially during the second half of the RP (150–400 yr CE). The onset of the RP was relatively cold and a 2.1˚C warming occurred during the first part of this period (0.8˚C 100 yr^{-1}). This SST evolution from colder to warmer conditions during the RP is consistent with the isotopic record from the Gulf of Taranto (Taricco et al., 2009) and peat reconstructions from north-western Spain (Martínez-Cortizas et al., 1999), and to some extend to SST proxies in the SE Tyrrhenian Sea (Lirer et al., 2014). However none of these records indicate that the RP was the warmest period of the last 2 kyr. Other records from higher latitudes such as Greenland (Dahl-Jensen et al., 1998), North Europe (Esper et al., 2014), North Atlantic Ocean (Bond et al., 2001; Sicre et al., 2008), speleothem records from North Iberia (Martín-Chivelet et al., 2011) and even the multiproxy PAGES 2K reconstruction from Europe, suggest a rather warmer early RP than late RP and, again, none of these records highlights the roman times as the warmest climate period of the last 2 kyr. Consequently, these very warm RP conditions recorded in the Minorca Mg/Ca-SST stack appears to have a very regional character and suggest a rather heterogeneous thermal response along the European continent and surrounding marine regions.

According to the δ^{18}Osw-stack the RP seems to be accompanied by an increase in the E–P ratio (Fig. 11a) as also has been observed in some close regions as Alps (Holzhauser et al., 2005; Joerin et al., 2006). But a lake record from Southern Spain indicates relatively high levels when δ^{18}Osw stack indicates the maximum in E–P ratio (Martín-Puertas et al., 2008). This information is not necessarily contradictory, since enhanced E–P balance in the Mediterranean could induce enhanced precipitation in some of the regions, but more detailed geographical information should be required to really evaluate such situation.

After the RP, during the whole DMA and until the MCA, Mg/Ca-SST stack shows a 2˚C cooling (-0.3˚C 100 yr^{-1}),, which is of 0.4˚C in the case of the Alkenone-SST stack; E–P rate is also decreasing. This trend is in contrast with the general warming trend interpreted in speleothem records from the North Iberia (Martín-Chivelet et al., 2011) or the transition towards drier conditions discussed from Alboran recods (Nieto- Moreno et al., 2011). SST proxies from the Tyrrhenian Sea show a cooling trend after the second half of the DMA and the Roman IV cold/dry phase described by Lirer et al. (2014) that can be tentatively correlated with our SST records (Fig. 11). This cooling phase is also documented in $\delta^{18}O_{G. ruber}$ record of Gulf of Taranto by Grauel et al. (2013). The heterogeneity of the signal in the different proxies and regions reveals the difficulty to characterise the climate variability during these short periods and reinforce the need of better geographical coverage of individual proxies.

Frequently, the Medieval Period is described as a very warm period in numerous regions in the Northern Hemisphere (Hughes and Diaz, 1994; Mann et al., 2008; Martín-Chivelet et al., 2011), but an increasing number of studies are questioning the existence of such a "warm" period (i.e. Chen et al., 2013). Minorca SST-stacks also indicate variable temperatures and it does not stand as a particular warm period within the last 2 kyr (Fig. 11). A significant warming event is centred at 900 yr CE and a later cooling with minimum values at about 1200 yr CE (Fig. 11). Higher variability is found in Greenland record (Kobashi et al., 2011) while an early warm MCA and posterior cooling is also observed in temperature reconstructions from Central Europe (Büntgen et al., 2011) and also the European multi-proxy 2k stack for PAGES 2K Consortium (2013). But all these proxies agree in indicating overall warmer temperatures during the MCA than during the LIA. At the MCA/LIA transition a progressive cooling and a change in cyclic oscillation before and after the onset of LIA are visible. This transition is considered the last rapid climate change (RCC) of Mayewski et al. (2004).

In the context of the Mediterranean Sea, lake, marine and speleothem proxies suggest drier conditions during the MCA than during the LIA (Moreno et al., 2012; Chen et al., 2013; Nieto-Moreno et al., 2013; Wassenburg et al., 2013). Looking to the δ^{18}Osw stack, several oscillations are observed during the MCA and LIA but any clear differentiation between the MCA and LIA can be inferred from this proxy, indicating that these reduced precipitation also involved reduced evaporation in the basin without altering the E–P balance recorded by the δ^{18}Osw proxy. The centennial scale variability detected in both the Mg/Ca-SST stack and δ^{18}Osw stack reveal that higher E–P conditions existed during the warmer intervals (Fig. 11a and c).

The LIA stands as a period of high thermal variability according to the Mg/Ca-SST stack and, in base to these records, two substages can be differentiated, a first one when SST oscillations were larger and average temperatures warmer (LIAa) and a second one with shorter oscillations and colder average SST (LIAb). We suggest that LIAa interval could be linked to the Wolf and Spörer solar minima and LIAb corresponds to Maunder and Dalton cold events, in agreement with previous observations (i.e. Vallefuoco et al., 2012).

Furthermore, the two LIA substages are also present in the Greenland record (Kobashi et al., 2011). The intense cooling drop (-1.0˚C 100 yr^{-1}) at the onset of the LIAb is in agreement with the suggested coolings of 0.5 and 1˚C in the Northern Hemisphere (i.e. Matthews and Briffa, 2005; Mann et al., 2009). The described two steps within the LIA are clearer in the Mg/Ca-SST stack than in the Alkenone-SST stack; this is also the case of the alkenone records in Alboran Sea (Nieto-Moreno et al., 2011) and may be consequence of the general reduced SST variability detected by these proxies (see Sect. 5.5).

In terms of humidity, the LIA is described as a period of increased runoff according to the Alboran record (Nieto-Moreno et al., 2011). The available lake level reconstruction from South Spain also reveals a progressive increase after the MCA, reaching a maximum during the LIAb (Martín-Puertas et al., 2008). Different records of flood events in the Iberia Peninsula also report a significant increase of extreme events during the LIA (Barriendos et al., 1998; Benito et al., 2003; Moreno et al., 2008). These conditions are consistent with the described enhanced storm activity over the GoL for the LIA (Sabatier et al., 2012). These conditions could account for the enhanced humidity transport towards the Mediterranean Sea that could produce the reduced E–P ratio detected in the δ^{18}Osw particularly for the LIAb (Fig. 11a).

The end of the LIA and onset of the IE is marked in the Mg/Ca-SST stack with a warming phase of about 1°C and less pronounced in the Alkenone-SST stack. This initial warm climatic event is also documented in other Mediterranean regions (Taricco et al., 2009; Marullo et al., 2011; Lirer et al., 2014) and Europe (PAGES 2K Consortium, 2013), which is coincident with a Total Solar Irradiance (TSI) enhancement after Dalton Minima. The two Minorca SST stacks show a cooling trend by the end of the record, which does not seem coherent with the instrumental atmospheric records. In Western Mediterranean, warming has been registered in two main phases: from the mid-1920s to 1950s and from the mid-1970s onwards (Lionello et al., 2006). The Minorca stacks do not show such a warming although they do not cover the second period of warming. Nevertheless, according to instrumental data from the upper layer on the Western Mediterranean since the beginning of the XX century, no warming trends were detected before the 1980s (Vargas-Yáñez et al., 2010).

6.2 Climate forcing mechanisms

The general cooling trend observed in both Mg/Ca-SST and Alkenone-SST stacks presents a good correlation with the summer insolation evolution in the North Hemisphere, which actually dominates the annual insolation balance (r=0.2 and 0.8, p value≤0.007, respectively) (Fig. 12). This external forcing has already been proposed to control major SST trends for the whole Holocene period in numerous records from Northern Hemisphere (i.e. Wright, 1994; Marchal et al., 2002; Kaufman et al., 2009; Moreno et al., 2012). Also summer insolation seems to have had a significant influence in the decreasing trend obtained in the isotope records during the whole spanned period (r=0.4, p value=0) as has been suggested in the study of Ausín et al. (2015), among others. Nevertheless, another forcing needs to account for the centennial-scale variability of the records as could be the higher volcanism in the last millennia (McGregor et al., 2015) although no significant correlations have been obtained between our records and volcanic reconstructions (Gao et al., 2008).

Solar variability has frequently been suggested as a primary driver of the Holocene millennial-scale variability (i.e. Bond et al., 2001). Several oscillations can be observed in the TSI record (Fig. 12a) whose correlation with the Mg/Ca-SST and Alkenone-SST stacks are low, since most of the major drops in TSI does not correspond to SST cold events; although in the case of the Alkenone-SST stack some degree of correlation exists between the two records (r=0.5, p value=0). Nevertheless, TSI does not seem to be the primer driver of the centennial scale SST variability in the studied records.

Furthermore, one of the major drivers of Mediterranean inter-annual variability in the Mediterranean region is the NAO (Hurrell, 1995; Lionello and Sanna, 2005; Mariotti, 2011). High state of the NAO produces high pressure over the Mediterranean Sea inducing an increment of the E–P balance and reduces sea level over several sectors of the Mediterranean Sea (Tsimplis and Josey, 2001). During these positive NAO periods, winds over the Mediterranean enhance their north direction, overall salinity increases and formation of dense deep water masses is reinforced as the water exchange through the Corsica channel while the arrival of north storm waves decreases (Wallace and Gutzler, 1981; Tsimplis and Baker, 2000; Lionello and Sanna, 2005). The effect of NAO on Mediterranean temperatures is more ambiguous. Changes during the last decades does not show significant variability with NAO (Luterbacher, 2004; Mariotti, 2011) although some studies suggest an opposite response between the two basins with cooling responses in some eastern basins and warming in the western during positive NAO conditions (Demirov and Pinardi, 2002; Tsimplis and Rixen, 2002). Although still controversial, some NAO reconstructions on proxy-records start to be available for the studied period (Lehner et al., 2012; Olsen et al., 2012; Trouet et al., 2012; Ortega et al., 2015). The last millennia are the best-resolved period and that allows a direct comparison with our data to evaluate the potential link to NAO.

The correlations between our Minorca temperatures stacks with NAO reconstructions (Fig. 12) are relatively low in the case of Mg/Ca-SST ($r=0.3$, p value≤ 0.002) and not significant in the Alkenone stack, indicating that this forcing is probably not the driver of the main trends in the records, although several uncertainties still exist about the long NAO reconstructions (Lehner et al., 2012). Notwithstanding the relatively low correlation between NAO with Mg/Ca-SST, when a detailed analysis is done focussing on the more intense negative NAO phases, those bellow 0 (Fig. 12), they mostly appear to correlate with cooling phases in the Mg/Ca-stack. The frequency of these negative events is particularly high during the LIA, and mostly during its second phase (LIAb) when the coldest intervals of our SST-stacks occurred.

When the last centuries are compared in detail with the last NAO reconstruction based on several different proxy records of annual resolution and tested with some model assimilations (Ortega et al., 2015), the obtained correlations between $\delta^{18}O_{sw}$ and NAO are not statistically significant. But Welch's test results indicate that the null hypothesis (difference between means is 0) cannot be discarded for both proxies, given that calculated p-value (0.913) is higher than the significance level alpha (0.05) ($t_{observed} = -0.109 < t_{critical} = 1.960$). During the last centuries it can be observed a coherent pattern of variability with our $\delta^{18}O_{SW}$ reconstruction, with high (low) isotopic values mainly dominating during positive (negative) NAO phases (Fig. 13). This picture is coherent with the described increase in the E–P balance during high NAO phases described for the last decades (Tsimplis and Josey, 2001), which would also contribute to the concentration of the ^{18}O in the Mediterranean waters. The SST stacks also suggest some degree o correlation between warm SST and high NAO values (Fig. 12) but a more coherent picture is observed when the SST-records are compared to the AMO reconstruction: warm SST dominated during high AMO values (Fig. 14). This picture of salinity changes related to NAO and SST to AMO has actually been also described in base to the analysis of last decades data (Mariotti, 2011; Guemas et al., 2014) and confirms the complex but tied response of the Mediterranean to atmospheric and marine changes over the North Atlantic Ocean.

The pattern of high $\delta^{18}O_{SW}$ when dominant positive NAO conditions occurred should indicate a reduction in the humidity transport over the Mediterranean region as a consequence of the high atmospheric pressure conditions (Tsimplis and Josey, 2001). To test this hypothesis, the $\delta^{18}O_{SW}$ stack and the NAO reconstruction is compared to a proxy interpreted to reflect storm intensity over the GoL (Fig. 13), also linked to increased storm activity in the Eastern North Atlantic (Sabatier et al., 2012). Several periods of increased/decreased storm activity in the GoL correlate indeed with low/high values in the $\delta^{18}O_{SW}$ supporting that during negative NAO conditions North European storm waves can more frequently arrive into the Mediterranean Sea (Lionello and Sanna, 2005), contributing to the reduction of the E–P balance (Fig. 13). This data comparison would also support that during these enhanced storm periods, cold SST conditions would dominate in the region as has been previously suggested (Sabatier et al., 2012). Nevertheless, not all the NAO oscillations had identical expression in the compared records and it is coherent with recent observations negative NAO phases that present different atmospheric configuration modes and thus impact over the western Mediterranean Sea (Sáez de Cámara et al., in proof, 2015). Regarding the lower part of the record, the maximum SST temperatures and $\delta^{18}O_{SW}$ recorded during the RP (100–300 yr CE) may suggest the occurrence of persistent positive NAO conditions, which would also be consistent with a high pressure driven drop in relatively sea level as has been reconstructed in the north-western Mediterranean Sea (Southern France) (-40 ± 10 cm) (Morhange et al., 2013).

It is interesting to note that during the DMA a pronounced and intense cooling event is recorded in the Mg/Ca-SST stack at about 500 yr CE. Several references document in the scientific literature the occurrence of the so-called dimming of the sun at 536–537 yr CE (Stothers, 1984). This event, in base to ice core records, has been able to be linked a tropical volcanic eruption (Larsen et al., 2008). Tree-ring data reconstructions from Europe and also historical documents indicate the persistence during several years (536–550 yr CE) of what is described as the most severe cooling across the Northern Hemisphere during the last two millennia (Larsen et al., 2008). Despite the limitations derived from the resolution of our records, Mg/Ca-SST stack record may have caught this cooling and that would prove the robustness of our age models.

7 Summary and conclusions

The review of new core top data of *G. bulloides*-Mg/Ca ratios from the central-western Mediterranean Sea together with previous published data support a consistent temperature sensitivity for the Mediterranean samples and allows to refine the previously calibrations. The recorded Mg/Ca-SST signal from *G. bulloides* is interpreted to reflect April–May conditions from the upper 40m layer. In contrast, the Alkenone-SST estimations are interpreted to integrate a more annual averaged signal, although biased toward the winter months since primary productivity during the summer months in the Mediterranean Sea is extremely low. This more averaged signal of the Alkenone-SST records may explain why they present more smoothed oscillations in comparison to the Mg/Ca-SST records.

After the careful construction of a common chronology for the studied multicores, in base to several chronological tools, the individual proxy records have been joined in an anomaly-stacked record to allow a better identification of the more solid patterns and structures. Both Alkenone and Mg/Ca-SST stacks show a consistent cooling trend over the studied period and since the Roman Period maxima this cooling is of about 2˚C in the alkenones record and 2.4˚C in the Mg/Ca record. This cooling trend seems to be consistent with the general lowering in summer insolation. This general cooling trend is punctuated by several SST oscillations at centennial time scale, which represent: maximum SST dominated during most of the Roman Period (RP); a progressive cooling during Dark Middle Ages (DMA); pronounced variability during Medieval Climate Anomaly (MCA) with two intense warming phases reaching warmer SST than during Little Ice Age (LIA); and very unstable and rather cold LIA, with two substages, a first one with larger SST oscillations and warmer average temperatures (LIAa) and a second one with shorter oscillations and colder average SST (LIAb). The described two stages within the LIA are clearer in the Mg/Ca-SST stack than in the Alkenone-SST record. Comparison of Mg/Ca-SST and $\delta^{18}O_{SW}$ stacks indicates that warmer intervals have been accompanied by higher Evaporation–Precipitation (E–P) conditions. The E–P balance oscillations over each defined climatic period during the last 2.7 kyr suggest variations in the thermal change and moisture export patterns in the central-western Mediterranean.

The comparison of the Minorca SST-stacks with other paleoclimatic records form Europe suggests a rather heterogonous thermal response along the European continent and surrounding marine regions. Comparison of the new Mediterranean records with the reconstructed variations in Total Solar Irradiance (TSI) does not support a clear connection with this climate forcing. Nevertheless, changes in the North Atlantic Oscillation (NAO) and Atlantic Multidecadal Oscillation (AMO) seem to have exerted a more relevant role controlling climate changes in the region. The negative NAO phases appear to correlate mostly with cooling phases in the Mg/Ca-stack, although this connection is complex and apparently clearer during the most intense negative phases. Nevertheless, when the comparison is focussed in the last 1 kyr, when NAO reconstructions are better constrained, a more consistent pattern arises, with cold and particularly fresher $\delta^{18}O_{SW}$ values (reduced E–P balance) during negative NAO phases. A picture of enhanced southward transport of European storm tracks during this period would be coherent with the new data and previous reconstructions of storm activity in the GoL. Nevertheless, the SST-stacks seem to present a more tied relation to AMO during the last four centuries (the available period of AMO reconstructions): warm SST dominated during high AMO values. These evidences would support a close connection between Mediterranean and North Atlantic oceanography for the last 2 kyr.

Acknowledgements. Cores MINMC06 were recovered by HERMES 3 cruise in 2006 on R/V Thethys II and HER-MC-MR3 cores were collected by HERMESIONE expedition on board of R/V Hespérides in 2009. This research has financially been supported by OPERA (CTM2013-48639-C2-1-R). We thank Generalitat de Catalunya Grups de Recerca Consolidats grant 2009 SGR 1305 to GRC Geociències Marines. Project of Strategic Interest NextData PNR 2011-2013 (www.nextdataproject.it) has also collaborated in the financing. We are grateful to M. Guart (Dept. d'Estratigrafia, Paleontologia i Geociències Marines, Universitat de Barcelona), M. Romero, T. Padró and J. Perona (Serveis Cientifico-Tècnics, Universitat de Barcelona), J.M. Bruach (Departament de Física, Universitat Autònoma de Barcelona) and B. Hortelano, Y. Gonzalez-Quinteiro and I. Fernández (Institut de Diagnosi Ambiental i Estudis de l'Aigua, CSIC, Barcelona) for their help with the laboratory work, D. Amblàs for his collaboration with the artwork of maps and to Paleoteam for the inconditional support. . L. Pena, S. Giralt and M. Blaauw are acknowledged for their help. B. Martrat acknowledges funding from CSIC-Ramon y Cajal post-doctoral program RYC-2013-14073. M. Cisneros benefited from a fellowship of the University of Barcelona. I. Cacho. thanks the ICREA-Academia program form the Generalitat de Catalunya.

References

Abrantes, F., Lebreiro, S., Rodrigues, T., Gil, I., Bartels-Jónsdóttir, H., Oliveira, P., Kissel, C., and Grimalt, J. O.: Shallow-marine sediment cores record climate variability and earthquake activity off Lisbon (Portugal) for the last 2000 years, Quaternary Sci. Rev., 24, 2477–2494, doi:10.1016/j.quascirev.2004.04.009, 2005.

Anand, P., Elderfield, H., and Conte, M. H.: Calibration of Mg/Ca thermometry in planktonic foraminifera from a sediment trap time series, Paleoceanography, 18, 1050, doi:10.1029/2002PA000846, 2003.

André, G., Garreau, P., Garnier, V., and Fraunié, P.: Modelled variability of the sea surface circulation in the North-western Mediterranean Sea and in the Gulf of Lions, Ocean Dynam., 55, 294–308, 2005.

Appleby, P. G. and Oldfield, F.: Application of Lead-210 to Sedimentation Studies, Clarendon Press, Oxford, Chapt. 21, 731–778, 1992.

Ausín, B., Flores, J. A., Sierro, F. J., Cacho, I., Hernández-Almeida, I., Martrat, B., and Grimalt, J. O.: Atmospheric patterns driving Holocene productivity in the Alboran Sea (Western Mediterranean): a multiproxy approach, The Holocene, 25, 1–13, doi:10.1177/0959683614565952, 2015.

Bárcena, M. A., Flores, J. A., Sierro, F. J., Pérez-Folgado, M., Fabres, J., Calafat, A., and Canals, M.: Planktonic response to main oceanographic changes in the Alboran Sea (Western Mediterranean) as documented in sediment traps and surface sediments, Mar. Micropaleontol., 53, 423–445, doi:10.1016/j.marmicro.2004.09.009, 2004.

Barker, S., Greaves, M., and Elderfield, H.: A study of cleaning procedures used for foraminiferal Mg/Ca paleothermometry, Geochem. Geophy. Geosy., 4, 9, doi:10.1029/2003GC000559, 2003.

Barker, S., Cacho, I., Benway, H., and Tachikawa, K.: Planktonic foraminiferal Mg/Ca as a proxy for past oceanic temperatures: a methodological overview and data compilation for the Last Glacial Maximum, Quaternary Sci. Rev., 24, 821–834, doi:10.1016/j.quascirev.2004.07.016, 2005.

Barriendos, M. and Martin-Vide, J.: Secular climatic oscillations as indicated by catastrophic floods in the spanish mediterranean coastal area (14th–19th centuries), Clim. Change, 38, 473–491, 1998.

Bé, A. W. H. and Hutson, W. H.: Ecology of planktonic foraminifera and biogeographic patterns of life and fossil assemblages in the Indian Ocean, Micropaleontology, 23, 369–414, 1977.

Bemis, B. E., Spero, H. J., Bijma, J. and Lea, D. W.: Reevaluation of the oxygen isotopic composition of planktonic foraminifera: Experimental results and revised paleotemperature equations, Paleoceanography, 13(2), 150–160, doi:10.1029/98PA00070, 1998.

Benito, G., Sopeña, A., Sánchez-Moya, Y., Machado, M. J., and Pérez-González, A.: Palaeoflood record of the Tagus River (Central Spain) during the Late Pleistocene and Holocene, Quaternary Sci. Rev., 22, 1737–1756, doi:10.1016/S0277-3791(03)00133-1, 2003.

Béthoux, J. P.: Mean water fluxes across sections in the Mediterranean Sea, evaluated in the basis of water and salt budgets and of observed salinities, Oceanol. Acta, 3, 79–88, 1980.

Blaauw, M. and Christen, J. A.: Flexible paleoclimate age-depth models using an autoregressive gamma process, Bayesian Anal., 6, 457–474, doi:10.1214/11-BA618, 2011.

Bond, G., Kromer, B., Beer, J., Muscheler, R., Evans, M. N., Showers, W., Hoffmann, S., Lottibond, R., Hajdas, I., and Bonani, G.: Persistent solar influence on North Atlantic climate during the holocene, Science, 294, 2130–2136, doi:10.1126/science.1065680, 2001.

Bosc, E., Bricaud, A., and Antoine, D.: Seasonal and interannual variability in algal biomass and primary production in the Mediterranean Sea, as derived from 4 years of SeaWiFS observations, Global Biogeochem. Cy., 18, 2003–2034, doi:10.1029/2003GB002034, 2004.

Boyle, E. A.: Manganese carbonate overgrowths on foraminifera tests, Geochim. Cosmochim. Ac., 47, 1815–1819, 1983.

Budillon F., Lirer F., Iorio M., Macri P., Sagnotti L., Vallefuoco M., Ferraro L., Innangi S., Sahabi M., Tonielli R.: Integrated stratigraphic reconstruction for the last 80 kyr in a deep sector of the Sardinia Channel (Western Mediterranean), Deep Sea Res Part II Top Stud. Oceanogr., 56, 725–737, 2009.

Büntgen, U., Tegel, W., Nicolussi, K., McCormick, M., Frank, D., Trouet, V., Kaplan, J. O., Herzig, F., Heussner, K. U., Wanner, H., Luterbacher, J., and Esper, J.: 2500 years of European climate variability and human susceptibility, Science, 331, 578–82, doi:10.1126/science.1197175, 2011.

Cacho, I., Pelejero, C., Grimalt, J. O., Calafat, A., and Canals, M.: C37 alkenone measurements of sea surface temperature in the Gulf of Lions (NW Mediterranean), Org. Geochem., 30, 557–566, 1999a.

Cacho, I., Grimalt, J. O., Pelejero, C., Canals, M., Sierro, F. J., Flores, J. A., and Shackleton, N.: Dansgaard-Oeschger and Heinrich event imprints in Alboran Sea paleotemperatures, Paleoceanography, 14, 698–705, 1999b.

Cacho, I., Grimalt, J. O., Sierro, F. J., Shackleton, N., and Canals, M.: Evidence for enhanced Mediterranean thermohaline circulation during rapid climatic coolings, Earth Planet. Sc. Lett., 183, 417–429, doi:10.1016/S0012-821X(00)00296-X, 2000.

Cacho, I., Grimalt, J., Canals, M., Sbaffi, L., Shackleton, N. J., Schönfeld, J., and Zahn, R.: Variability of the western Mediterranean Sea surface temperature during the last 25,000 years ans its connection with the Northern Hemisphere climatic changes, Paleoceanography, 16, 40–52, 2001.

Cacho, I., Shackleton, N., Elderfield, H., Sierro, F. J. and Grimalt, J. O.: Glacial rapid variability in deep-water temperature and $\delta^{18}O$ from the Western Mediterranean Sea, Quat. Sci. Rev., 25, 3294–3311, doi:10.1016/j.quascirev.2006.10.004, 2006.

Calafat, A. M., Casamor, J., Canals, M., and Ny_ eler, F.: Distribución y composición elemental de la materia particulada en suspensión en el Mar Catalano-Balear, Geogaceta, 20, 370–373, 1996.

Calvert, S. and Pedersen, T.: Sedimentary geochemistry of manganese: implications for the environment of formation of manganiferous black shales, Econ. Geol., 91, 36–47, 1996.

Canals, M., Puig, P., Madron, X. D. De, Heussner, S., Palanques, A., and Fabres, J.: Flushing submarine canyons, Nature, 444, 354–357, doi:10.1038/nature05271, 2006.

Chen, L., Zonneveld, K. A. F., and Versteegh, G. J. M.: The Holocene Paleoclimate of the Southern Adriatic Sea region during the “Medieval Climate Anomaly” reflected by organic walled dinoflagellate cysts, The Holocene, 23, 645–655, doi:10.1177/0959683612467482, 2013.

Cléroux, C., Cortijo, E., Anand, P., Labeyrie, L., Bassinot, F., Caillon, N., and Duplessy, J. C.: Mg/Ca and Sr/Ca ratios in planktonic foraminifera: proxies for upper water column temperature reconstruction, Paleoceanography, 23, PA3214, doi:10.1029/2007PA001505, 2008.

Combourieu Nebout, N., Turon, J., Zahn, R., Capotondi, L., Londeix, L., and Pahnke, K.: Enhanced aridity and atmospheric high-pressure stability over the western Mediterranean during the North Atlantic cold events of the past 50 k.y., Geology, 30, 863–866, 2002.

Combourieu Nebout, N., Peyron, O., Dormoy, I., Desprat, S., Beaudouin, C., Kotthoff , U., and Marret, F.: 5 Rapid climatic variability in the west Mediterranean during the last 25 000 years from high resolution pollen data, Clim. Past, 5, 503–521, doi:10.5194/cp-5-503-2009, 2009.

Conte, M. H., Sicre, M. A., Rühlemann, C., Weber, J. C., Schulte, S., Schulz-Bull, D., and Blanz, T.: Global temperature calibration of the alkenone unsaturation index ($U^{K'}_{37}$) in surface waters and comparison with surface sediments, Geochem. Geophy. Geosy., 7, 2, doi:10.1029/2005GC001054, 2006.

Coplen, T.: New guidelines for reporting stable hydrogen, carbon, and oxygen isotope-ratio data, Geochim. Cosmochim. Ac., 60, 3359–3360, 1996.

Corella, J. P., Moreno, A., Morellón, M., Rull, V., Giralt, S., Rico, M. T., Pérez-Sanz, A., and Valero-Garcés, B. L.: Climate and human impact on a meromictic lake during the last 6000 years (Montcortés Lake, Central Pyrenees, Spain), J. Palaeolimnol., 46, 351–367, 2011.

Craig, H.: The measurement of oxygen isotope paleotemperatures, in: Stable Isotopes in Oceanographic Studies and Paleotemperatures, edited by: Tongiorgi, E., Consiglio Nazionale delle Ricerche, Laboratorio di Geologia Nucleare, Pisa, 1–24, 1965.

D'Ortenzio, F. and Ribera d'Alcalà, M.: On the trophic regimes of the Mediterranean Sea: a satellite analysis, Biogeosciences, 6, 139–148, doi:10.5194/bg-6-139-2009, 2009.

Dahl-Jensen, D., Mosegaard, K., Gundestrup, N., Clow, G. D., Johnses, S. J., Hansen, A. W., and Balling, N.: Past temperatures directly from the Greenland ice sheet, Science, 282, 268–271, 1998.

Demirov, E. and Pinardi, N.: Simulation of the Mediterranean Sea circulation from 1979 to 1993: Part I. The interannual variability, J. Marine Syst., 33–34, 23–50, 2002.

Di Bella, L., Frezza, V, Bergamin, L., Carboni, M. G., Falese, F., Mortorelli, E., Tarragoni, C., and Chiocci, F. L.: Foraminiferal record and high-resolution seismic stratigraphy of the Late Holocene succession of the submerged Ombrone River delta (Northern Tyrrhenian Sea, Italy), Quatern. Int., 328–329, 287–300, 2014.

Eglinton, T. I., Conte, M. H., Eglinton, G., and Hayes, J. M.: Proceedings of a workshop on alkenone-based paleoceanographic indicators, Geochem. Geophy. Geosy., 2, 1, doi:10.1029/2000GC000122, 2001.

Elderfield, H. and Ganssen, G.: Past temperature and $\delta^{18}O$ of surface ocean waters inferred from foraminiferal Mg/Ca ratios, Nature, 405, 442–445, 2000.

Esper, J., Frank, D. C., Büntgen, U., Verstege, A., Luterbacher, J., and Xoplaki, E.: Long-term drought severity variations in Morocco, Geophys. Res. Lett., 34, L17702, doi:10.1029/2007GL030844, 2007.

Esper, J., Düthorn, E., Krusic, P. J., Timonen, M., and Büntgen, U.: Northern European summer temperature variations over the Common Era from integrated tree-ring density records, J. Quat. Sci., 29, 487–494, doi:10.1002/jqs.2726, 2014.

Estrada, M., Vives, F., and Alcaraz, M.: Life and productivity in the open sea, in: Western Mediterranean, edited by: Margalef, R., Oxford, Pergamon Press, 148–197, 1985.

Fanget, A. S., Bassetti, M. A., Arnaud, M., Chi_ oleau, J. F., Cossa, D., Goineau, A.,Fontanier, C., Buscail, R., Jouet, G., Maillet, G. M., Negri, A., Dennielou, B., and Berné, S.: Historical evolution and extreme climate events during the last 400 years on the Rhone prodelta (NW Mediterranean), Mar. Geol., 346, 375–391, doi:10.1016/j.margeo.2012.02.007, 2013.

Ferguson, J. E., Henderson, G. M., Kucera, M., and Rickaby, R. E. M.: Systematic change of foraminiferal Mg/Ca ratios across a strong salinity gradient, Earth Planet. Sc. Lett., 265,153–166, doi:10.1016/j.epsl.2007.10.011, 2008.

Fleitmann, D., Cheng, H., Badertscher, S., Edwards, R. L., Mudelsee, M., G.ktürk, O. M., Fankhauser, A., Pickering, R., Raible, C. C., Matter, A., Kramers, J., and Tüysüz, O.: Timing and climatic impact of Greenland interstadials recorded in stalagmites from northern Turkey, Geophys. Res. Lett., 36, L19707, doi:10.1029/2009GL040050, 2009.

Fletcher, W. J. and Sánchez Goñi, M. F.: Orbital and sub-orbital-scale climate impacts on vegetation of the western Mediterranean basin over the last 48 000 yr, Quaternary Res., 70, 451–464, 2008.

Fletcher, W. J., Debret, M., and Sanchez Goñi, M.: Mid-Holocene emergence of a low-frequency millennial oscillation in western Mediterranean climate: implications for past dynamics of the North Atlantic atmospheric westerlies, The Holocene, 23, 153–166, doi:10.1177/0959683612460783, 2012.

Frigola, J.: Variabilitat climàtica ràpida a la conca occidental del Mediterrani: registre sedimentològic, Ph.D. Thesis, Dept. of Stratigraphy, Paleontology and Marine Geosciences, University of Barcelona, Spain, 2012.

Frigola, J., Moreno, A., Cacho, I., Canals, M., Sierro, F. J., Flores, J. A., Grimalt, J. O., Hodell, D. A., and Curtis, J. H.: Holocene climate variability in the western Mediterranean region from a deepwater sediment record, Paleoceanography, 22, PA2209, doi:10.1029/2006PA001307, 2007.

Frigola, J., Moreno, A., Cacho, I., Canals, 5 M., Sierro, F. J., Flores, J. A., and Grimalt, J. O.: Evidence of abrupt changes in Western Mediterranean Deep Water circulation during the last 50 kyr: a high-resolution marine record from the Balearic Sea, Quatern. Int., 181, 88–104, doi:10.1016/j.quaint.2007.06.016, 2008.

Frisia, S., Borsato, A., Preto, N., and McDermott, F.: Late Holocene annual growth in three Alpine stalagmites records the influence of solar activity and the North Atlantic Oscillation on winter climate, Earth Planet. Sci. Lett., 216, 411–424, 2003.

Ganssen, G. M. and Kroon, D.: The isotopic signature of planktonic foraminifera from NE Atlantic surface sediments: implications for the reconstruction of past oceanic conditions, J. Geol. Soc. London, 157, 693–699, 2000.

Gao, C., Robock, A. and Ammann, C.: Volcanic forcing of climate over the past 1500 years: An improved ice core-based index for climate models, J. Geophys. Res., 113, D23111, doi:10.1029/2008JD010239, 2008.

Garcia-Orellana, J., Pates, J. M., Masqué, P., Bruach, J. M., and Sanchez-Cabeza, J. A.: Distribution of artificial radionuclides in deep sediments of the Mediterranean Sea, Sci. Total Environ., 407, 887–98, doi:10.1016/j.scitotenv.2008.09.018, 2009.

Giorgi, F.: Climate change hot-spots, Geophys. Res. Lett., 33, L08707, doi:10.1029/2006GL025734, 2006.

Goudeau, M. L. S., Reichart, G. J., Wit, J. C., de Nooijer, L. J., Grauel, A. L., Bernasconi, S. M., and de Lange, G. J.: Seasonality variations in the Central Mediterranean during climate change events in the Late Holocene, Palaeogeogr. Palaeocl., 418, 304–318, 2015.

Goy, J. L, Zazo, C., and Dabrio, C. J.: A beach-ridge progradation complex reflecting periodical sea-level and climate variability during the Holocene (Gulf of Almeria, Western Mediterranean), Geomorphology, 50, 251–268, 2003.

Gray, S. T., Graumlich, L. J., Betancourt, J. L., and Pederson, G. T.: A tree-ring based reconstruction of the Atlantic Multidecadal Oscillation since 1567 A. D., Geophys. Res. Lett., 31,12, doi:10.1029/2004GL019932, 2004.

Griggs, C., DeGaetano, A., Kuniholm, P., and Newton, M.: A regional high-frequency reconstruction of May–June precipitation in the north Aegean from oak tree rings, AD 1089–1989, Int. J. Climatol., 27, 1075–1089, 2007.

Grauel, A. L., Goudeau, M. L. S., de Lange, G. J., and Bernasconi, S. M.: Climate of the past 2500 years in the Gulf of Taranto, central Mediterranean Sea: a high-resolution climate reconstruction based on $\delta^{18}O$ and $\delta^{13}C$ of *Globigerinoides ruber* (white), The Holocene, 23,1440–1446, doi:10.1177/0959683613493937, 2013.

Guemas, V., García-Serrano, J., Mariotti, A., Doblas-Reyes, F., and Caron, L. P.: Prospects for decadal climate prediction in the Mediterranean region, Q. J. Roy. Meteor. Soc., 141, 580–597, doi:10.1002/qj.2379, 2014.

Hernández-Almeida, I., Bárcena, M. Á., Flores, J. A., Sierro, F. J., Sánchez-Vidal, A., and Calafat, A.: Microplankton response to environmental conditions in the Alboran Sea (Western Mediterranean): one year sediment trap record, Mar. Micropaleontol., 78, 14–24, doi:10.1016/j.marmicro.2010.09.005, 2011.

Holzhauser, H., Magny, M., and Heinz, J.: Glacier and lake-level variations in west-central Europe over the last 3500 years, The Holocene, 15, 789–801, 2005.

Hönisch, B., Allen, K. A., Lea, D. W., Spero, H. J., Eggins, S. M., Arbuszewski, J., DeMenocal, P., Rosenthal, Y., Russell, A. D., and Elderfield, H.: The influence of salinity on Mg/Ca in planktic foraminifers – evidence from cultures, core-top sediments and complementary $\delta^{18}O$, Geochim. Cosmochim. Ac.,121, 196–213, 2013.

Hoogakker, B. A. A., Klinkhammer, G. P., Elderfield, H., Rohling, E. J., and Hayward, C.: Mg/Ca paleothermometry in high salinity environments, Earth Planet. Sc. Lett., 284, 583–589, doi:10.1016/j.epsl.2009.05.027, 2009.

Huang, S.: Merging information from different resources for new insights into climate change in the past and future, Geophys. Res. Lett., 31, 1–4, doi:10.1029/2004GL019781, 2004.

Hughes, M. K. and Diaz, H. F.: Was there a "Medieval warm period", and if so, where and when?, Clim. Change, 109–142, 1994.

Hurrell, J. W.: Decadal Trends in the North Atlantic Oscillation: regional temperatures and precipitation, Science, 269, 676–679, doi:10.1126/science.269.5224.676, 1995.

Incarbona, A., Ziveri, P., Di Stefano, E., Lirer, F., Mortyn, G., Patti, B., Pelosi, N., Sprovieri, M., Tranchida, G., Vallefuoco, M., Albertazzi, S., Bellucci, L. G., Bonanno, A., Bonomo, S., Censi, P., Ferraro, L., Giuliani, S., Mazzola, S., and Sprovieri, R.: The Impact of the Little Ice Age on Coccolithophores in the Central Mediterranea Sea, Clim. Past, 6, 795–805, doi:10.5194/cp-6-795-2010, 2010.

Jalut, G., Esteban Amat, A., Mora, S. R., Fontugne, M., Mook, R., Bonnet, L., and Gauquelin, T.: Holocene climatic changes in the western Mediterranean: installation of the Mediterranean climate, CR. Acad. Sci. Ser. II, 325, 327–334, 1997.

Jalut, G., Esteban Amat, A., Bonnet, L., Gauquelin, T., and Fontugne, M.: Holocene climatic changes in the Western Mediterranean, from south-east France to south-east Spain, Palaeogeogr. Palaeocl., 160, 255–290, 2000.

Joerin, U. E., Stocker, T. F., Schlu, C., and Physics, E.: Multicentury glacier fluctuations in the Swiss Alps during the Holocene, The Holocene, 16, 697–704, 2006.

Kaufman, D. S., Schneider, D. P., McKay, N. P, Ammann, C. M., Bradley, R. S., Bri_ a, K. R., Miller, G. H., Otto-Bliesner, B. L., Overpeck, J. P., and Vinther, B. M.: Recent warming reverses long-term arctic cooling, Science, 325, 1236–1239, doi:10.1126/science.1173983, 2009.

Kobashi, T., Kawamura, K., Severinghaus, J. P., Barnola, J. M., Nakaegawa, T., Vinther, B. M., Johnsen, S. J., and Box, J. E.: High variability of Greenland surface temperature over the past 4000 years estimated from trapped air in an ice core, Geophys. Res. Lett., 38, 21, doi:10.1029/2011GL049444, 2011.

Krishnaswami, S., Lal, D., Martin, J. M., and Meybeck, M.: Geochronology of lake sediments, Earth. Planet. Sci. Lett, 11, 407–414, 1971.

Labuhn, I., Genty, D., Vonhof, H., Bourdin, C., Blamart, D., Douville, E., Ruan, J., Cheng, H., Edwards, R. L., Pons-Branchu, E., and Pierre, M.: A high-resolution fluid inclusion $\delta^{18}O$ record from a stalagmite in SW France: modern calibration and comparison with multiple proxies, Quaternary Sci. Rev., 110, 152–165, doi:10.1016/j.quascirev.2014.12.021, 2015.

Lacombe, H., Gascard, J. C, Cornella, J., and Béthoux, J. P.: Response of the Mediterranean to the water and energy fluxes across its surface, on seasonal and interannual scales, Oceanol. Acta, 4, 247–255, 1981.

Lacombe, H., Tchernia, P., and Gamberoni, L.: Variable bottom water in the Western Mediterranean basin, Prog. Oceanogr., 14, 319–338, 1985.

Larsen, L. B., Vinther, B. M., Bri_ a, K. R., Melvin, T. M., Clausen, H. B., Jones, P. D., Siggaard-Andersen, M. L., Hammer, C. U., Eronen, M., Grudd, H., Gunnarson, B. E., Hantemirov, R. M., Naurzbaev, M. M., and Nicolussi, K.: New ice core evidence for a volcanic cause of the A.D. 536 dust veil, Geophys. Res. Lett., 35, 1–5, doi:10.1029/2007GL032450, 2008.

Laskar, J., Robutel, P., Joutel, F., Gastineau, M., Correia, A. C. M., and Levrard, B.: A longterm numerical solution for the insolation quantities of the Earth, Astron. Astrophys., 285, 261–285, 2004.

Lea, D. W., Mashiotta, T. A., and Spero, H. J.: Controls on magnesium and strontium uptake in planktonic foraminifera determined by live culturing, Geochim. Cosmochim. Ac., 63, 2369–2379, 1999.

Lea, D. W., Pak, D. K., and Paradis, G.: Influence of volcanic shards on foraminiferal Mg/Ca in a core from the Galápagos region, Geochem. Geophy. Geosy., 6, 11, doi:10.1029/2005GC000970, 2005.

Lebreiro, S. M., Francés, G., Abrantes, F. F. G., Diz, P., Bartels-Jónsdóttir, H. B., Stroynowski, Z. N., Gil, I. M., Pena, L. D., Rodrigues, T., Jones, P. D., Nombela, M. A., Alejo, I., Bri_ a, K. R., Harris, I., and Grimalt, J. O.: Climate change and coastal hydrographic response along the Atlantic Iberian margin (Tagus Prodelta and Muros Ría) during the last two millennia, The Holocene, 16, 1003–1015, 2006.

Lehner, F., Raible, C. C., and Stocker, T. F.: Testing the robustness of a precipitation proxy-based North Atlantic Oscillation reconstruction, Quaternary Sci. Rev., 45, 85–94, doi:10.1016/j.quascirev.2012.04.025, 2012.

Lionello, P.: The Climate of the Mediterranean Region: From the Past to the Future, Elsevier Science, Burlington, MA, 2012.

Lionello, P. and Sanna, A.: Mediterranean wave climate variability and its links with NAO and Indian Monsoon, Clim. Dynam., 25, 611–623, doi:10.1007/s00382-005-0025-4, 2005.

Lionello, P., Malanott-Rizzoli, R., Boscolo, R., Alpert, P., Artale, V., Li, L., Luterbacher, J., May, W., Trigo, R., Tsimplis, M., Ulbrich, U., and Xoplaki, E.: The Mediterranean climate: An overview of the main characteristics and issues, in:

Mediterranean Climate Variability (MedClivar), Elsevier, Amsterdam, 1–26, 2006.

Lirer, F., Sprovieri, M., Ferraro, L., Vallefuoco, M., Capotondi, L., Cascella, A., Petrosino, P., Insinga, D. D., Pelosi, N., Tamburrino, S., and Lubritto, C.: Integrated stratigraphy for the Late Quaternary in the eastern Tyrrhenian Sea, Quatern. Int., 292, 71–85, doi:10.1016/j.quaint.2012.08.2055, 2013.

Lirer, F., Sprovieri, M., Vallefuoco, M., Ferraro, L., Pelosi, N., Giordano, L., and Capotondi, L.: Planktonic foraminifera as bio-indicators for monitoring the climatic changes that have occurred over the past 2000 years in the southeastern Tyrrhenian Sea, Integr. Zool., 9, 542–54, doi:10.1111/1749-4877.12083, 2014.

Luterbacher, J., Dietrich, D., Xoplaki, E., Grosjean, M., andWanner, H.: European seasonal and annual temperature variability, trends, and extremes since 1500, Science, 303, 1499–1503, doi:10.1126/science.1093877, 2004.

Malanotte-Rizzoli, P., Artale, V., Borzelli-Eusebi, G. L., Brenner, S., Crise, A., Gacic, M., Kress, N., Marullo, S., Ribera d'Alcalà, M., Sofianos, S., Tanhua, T., Theocharis, A., Alvarez, M., Ashkenazy, Y., Bergamasco, A., Cardin, V., Carniel, S., Civitarese, G., D'Ortenzio, F., Font, J., Garcia-Ladona, E., Garcia-Lafuente, J. M., Gogou, A., Gregoire, M., Hainbucher, D., Kontoyannis, H., Kovacevic, V., Kraskapoulou, E., Kroskos, G., Incarbona, A., Mazzocchi, M. G., Orlic, M., Ozsoy, E., Pascual, A., Poulain, P.-M., Roether, W., Rubino, A., Schroeder, K., Siokou-Frangou, J., Souvermezoglou, E., Sprovieri, M., Tintoré, J., and Triantafyllou, G.: Physical forcing and physical/biochemical variability of the Mediterranean Sea: a review of unresolved issues and directions for future research, Ocean Sci., 10, 281–322, doi:10.5194/os-10-281-2014, 2014.

Maldonado, A., Got, H., Monaco, A., O'Connell, S., and Mirabile, L.: Valencia Fan (northwestern Mediterranean): distal deposition fan variant, Mar. Geol., 62, 295–319, 1985.

Mangini, A., Spötl, C., and Verdes, P.: Reconstruction of temperature in the Central Alps during the past 2000 yr from a $\delta^{18}O$ stalagmite record, Earth. Planet. Sci. Lett., 235, 741–751, 2005.

Mann, M. E., Zhang, Z., Hughes, M. K., Bradley, R. S., Miller, S. K., Rutherford, S., and Ni, F.: Proxy-based reconstructions of hemispheric and global surface temperature variations over the past two millennia, P. Natl. Acad. Sci. USA, 105, 13252–13257, 2008.

Mann, M. E., Zhang, Z., Rutherford, S., Bradley, R. S., Hughes, M. K., Shindell, D., Ammann, C., Faluvegi, G., and Ni, F.: Global signatures and dynamical origins of the little ice age and medieval climate anomaly, Science, 326, 1256–1260, 2009.

Marchal, O., Cacho, I., Stocker, T. F., Grimalt, J. O., Calvo, E., Martrat, B., Shackleton, N., Vautravers, M., Cortijo, E., Van Kreveld, S., Andersson, C., Ko, N., Chapman, M., Sbaffi, L., Duplessy, J., Sarnthein, M., and Turon, J.: Apparent long-term cooling of the sea surface in the northeast Atlantic and Mediterranean during the Holocene, Quaternary Sci. Rev., 21, 455–483, 2002.

Margaritelli G., Lirer F., Vallefuoco M., Bonomo S., Cascella A., Capotondi L., Ferraro L., Insinga D.D., Petrosino P., Rettori R.: Climatic variability during the last two millennia in the Tyrrhenian Sea: evidences from planktonic foraminifera and geochemical data, XV Edizione delle "Giornate di Paleontologia" PALEODAYS2015, Palermo 17-29 Maggio 2015, 72-73. Società Paleontologica Italiana, 2015.

Mariotti, A.: Decadal climate variability and change in the Mediterranean Region, Sci. Technol. Infus. Clim. Bull., Climate Test Bed Joint Seminar Series, Maryland, US National Oceanic and Atmospheric Administration, 1–5, 2011.

Martin, J., Elbaz-Poulichet, F., Guieu, C., Lo¸ e-Pilot, M., and Han, G.: River versus atmospheric input of material to the Mediterranean Sea: an Overview, Mar. Chem., 28, 159–182, 1989.

Martín-Chivelet, J., Muñoz-García, M. B., Edwards, R. L., Turrero, M. J., and Ortega, A. I.: Land surface temperature changes in Northern Iberia since 4000 yr BP, based on $\delta^{13}C$ of speleothems, Glob. Planet. Change., 77, 1–12, doi:10.1016/j.gloplacha.2011.02.002, 2011.

Martín-Puertas, C., Valero-Garcés, B. L., Brauer, A., Mata, M. P., Delgado-Huertas, A., and Dulski, P.: The Iberian–Roman Humid Period (2600–1600 cal yr BP) in the Zoñar Lake varve record (Andalucía, Southern Spain), Quaternary Res., 71, 2, doi:10.1016/j.yqres.2008.10.004, 2008.

Martínez-Cortizas, A., Pontevedra-Pombal, X., García-Rodeja, E., Nóvoa-Muñoz, J. C., and Shotyk, W.: Mercury in a Spanish Peat Bog: archive of climate change and atmospheric metal deposition, Science, 284, 939–942, 1999.

Martrat, B., Grimalt, J. O., Lopez-Martinez, C., Cacho, I., Sierro, F. J., Flores, J. A., Zahn, R., Canals, M., Curtis, J. H., and Hodell, D. A.: Abrupt temperature changes in the Western Mediterranean over the past 250 000 years, Science, 306, 1762, doi:10.1126/science.1101706, 2004.

Marullo, S., Artale, V., and Santoleri, R.: The SST multi-decadal variability in the Atlantic-Mediterranean region and its relation to AMO, J. Climate, 24, 4385–4401, doi:10.1175/2011JCLI3884.1, 2011.

Mashiotta, T. A., Lea, D. W., and Spero, H. J.: Glacial–interglacial changes in Subantarctic sea surface temperature and $\delta^{18}O$-water using foraminiferal Mg, Earth Planet. Sc. Lett., 170, 417–432, 1999.

Masqué, P., Fabres, J., Canals, M., Sanchez-Cabeza, J. A., Sanchez-Vidal, A., Cacho, I., Calafat, A. M., and Bruach, J. M.: Accumulation rates of major constituents of hemipelagic sediments in the deep Alboran Sea: a centennial perspective of sedimentary dynamics, Mar. Geol., 193, 207–233, 2003.

Matthews, J. A. and Bri_ a, K. R.: The “Little ice age”: re-evaluation of an evolving concept, Geogr. Ann. A, 87, 17–36, 2005.

Mauffret, A.: Etude géodynamique de la marge des Illes Baléares, Mémoires de la Société Géologique de France LVI, 1–96, 1979.

Mayewski, P. A., Rohling, E. E., Stager, J. C., Karlen, W., Maasch, K. A., Meeker, L. D., Meyerson, E. A., Gasse, F., van Kreveld, S., Holmgren, K., Lee-Thorp, J., Rosqvist, G. Rack, F., Staubwasser, M., Schneider, R. R., and Steig, E. J.: Holocene climate variability, Quaternary Res., 62, 243–255, 2004.

McConnell, M. C. and Thunell, R. C.: Calibration of the planktonic foraminiferal Mg/Ca paleothermometer: sediment trap results from the Guaymas Basin, Gulf of California, Paleoceanography, 20, PA2016, doi:10.1029/2004PA001077, 2005.

McGregor, H. V., Evans, M. N., Goosse, H., Leduc, G., Martrat, B., Addison, J. A., Graham Mortyn, P., Oppo, D. W., Seidenkrantz, M.-S., Sicre, M.-A., Phipps, S. J., Selvaraj, K., Thirumalai, K., Filipsson, H. L. and Ersek, V.: Robust global ocean cooling trend for the pre-industrial Common Era, Nat Geosci, 8(9), 671–677, doi:10.1038/ngeo2510, 2015.

MEDAR GROUP, MEDATLAS/2002 European Project: Mediterranean and Black Sea Database of Temperature Salinity and Bio-Chemical Parameters, Climatological Atlas, Institut Français de Recherche pour L’Exploitation de la Mer (IFREMER), Edition/Instituto Nazionale di Oceanografia e di Geofisica Sperimentale (OGS), 2002.

Medoc, G.: Observation of formation of Deep Water in the Mediterranean Sea, Nature, 227, 1037–1040, 1970.

Millán, M. M., Estrela, M. J., Sanz, M. J., Mantilla, E., Martín, M., Pastor, F., Salvador, R., Vallejo, R., Alonso, L., Gangoiti, G., Ilardia, J. L., Navazo, M., Albizuri, A., Artiñano, B., Ciccioli, P., Kallos, G., Carvalho, R. A., Andrés, D., Ho_ , A., Werhahn, J., Seufert, G., and Versino, B.: Climatic feedbacks and desertification: the Mediterranean Model, J. Climate, 18, 684–701, 2005.

Millot, C.: Circulation in the Western Mediterranean Sea, J. Marine Syst., 20, 423–442, 1999.

Morellón, M., Pérez-Sanz, A., Corella, J. P., Büntgen, U., Catalán, J., González-Sampériz, P., González-Trueba, J. J., López-Sáez, J. A., Moreno, A., Pla-Rabes, S., Saz-Sánchez, M. Á., Scussolini, P., Serrano, E., Steinhilber, F., Stefanova, V., Vegas-Vilarrúbia, T., and Valero-Garcés, B.: A multi-proxy perspective on millennium-long climate variability in the Southern Pyrenees, Clim. Past, 8, 683–700, doi:10.5194/cp-8-683-2012, 2012.

Moreno, A., Cacho, I., Canals, M., Prins, M. A., Sánchez-Goñi, M. F., Grimalt, J. O., and Weltje, G. J.: Saharan Dust Transport and High-Latitude Glacial Climatic Variability: the Alboran Sea Record, Quaternary Res., 58, 318–328, doi:10.1006/qres.2002.2383, 2002.

Moreno, A., Cacho, I., Canals, M., Grimalt, J. O., Sánchez-Goñi, M. F., Shackleton, N., and Sierro, F. J.: Links between marine and atmospheric processes oscillating on a millennial time-scale. A multi-proxy study of the last 50,000 yr from the Alboran Sea (Western Mediterranean Sea), Quaternary Sci. Rev., 24, 1623–1636, doi:10.1016/j.quascirev.2004.06.018, 2005.

Moreno, A., Valero-Garcés, B. L., González-Sampériz, P., and Rico, M.: Flood response to rainfall variability during the last 2000 years inferred from the Taravilla Lake record (Central Iberian Range, Spain), J. Paleolimnol., 40, 943–961, doi:10.1007/s10933-008-9209-3, 2008.

Moreno, A., Pérez, A., Frigola, J., Nieto-Moreno, V., Rodrigo-Gámiz, M., Martrat, B., González-Sampériz, P., Morellón, M., Martín-Puertas, C., Pablo, J., Belmonte, Á., Sancho, C., Cacho, I., Herrera, G., Canals, M., Grimalt, J. O., Jiménez-Espejo, F., Martínez-Ruiz, F., Vegas-Vilarrúbia, T., and Valero-Garcés, B. L.: The Medieval Climate Anomaly in the Iberian Peninsula reconstructed from marine and lake records, Quaternary Sci. Rev., 43, 16–32, doi:10.1016/j.quascirev.2012.04.007, 2012.

Morhange, C., Marriner, N., Excoffon, P., Bonnet, S., Flaux, C., Zibrowius, H., Goiran, J. P., and El Amouri, M.: Relative Sea-Level Changes During Roman Times in the Northwest Mediterranean: the 1st Century AD. Fish Tank of Forum Julii, Fréjus, France, Geoarchaeology, 28, 363–372, doi:10.1002/gea.21444, 2013.

Mulitza, S., Boltovskoy, D., Donner, B., Meggers, H., Paul, A. and Wefer, G.: Temperature: δ 18O relationships of planktonic foraminifera collected from surface waters, Palaeogeogr Palaeoclimatol Palaeoecol, 202(1-2), 143–152, doi:10.1016/S0031-0182(03)00633-3, 2003.

Nieto-Moreno, V., Martínez-Ruiz, F., Giralt, S., Jiménez-Espejo, F., Gallego-Torres, D., Rodrigo-Gámiz, M., García-Orellana, J., Ortega-Huertas, M., and de Lange, G. J.: Tracking climate variability in the western Mediterranean during the Late Holocene: a multiproxy approach, Clim. Past, 7, 1395–1414, doi:10.5194/cp-7-1395-2011, 2011.

Nieto-Moreno, V., Martínez-Ruiz, F., Willmott, V., García-Orellana, J., and Masqué, P.: Organic geochemistry climate conditions in the westernmost Mediterranean over the last two millennia: an integrated biomarker approach, Org. Geochem., 55, 1–10,

doi:10.1016/j.orggeochem.2012.11.001, 2013.
Olsen, J., Anderson, N. J., and Knudsen, M. F.: Variability of the North Atlantic Oscillation over the past 5200 years, Nat. Geosci., 5, 808–812, doi:10.1038/ngeo1589, 2012.
Ortega, P., Lehner, F., Swingedouw, D., Masson-Delmotte, V., Raible, C. C., Casado, M., and Yiou, P.: A model-tested North Atlantic Oscillation reconstruction for the past millennium, Nature, 523, 7558, doi:10.1038/nature14518, 2015.
PAGES: Science Plan and Implementation Strategy, IGBP Report No. 57, IGBP Secretariat, Stockholm, 2009.
PAGES 2K Consortium: Continental-scale temperature variability during the past two millennia, Nature, 6, 339–346, doi:10.1038/NGEO1797, 2013.
Pastor, F.: Ciclogénesis intensas en la cuenca occidental del Mediterráneo y temperatura superficial del mar: modelización y evaluación de las áreas de recarga, PhD Thesis, Dept. of Astronomy and Meteorology, University of Barcelona, Spain, 2012.
Pastor, F., Estrela, M., Peñarrocha, D., and Millán, M.: Torrential rains on the Spanish Mediterranean Coast: modeling the effects of the sea surface temperature, J. Appl. Meteorol., 40, 1180–1195, 2001.
Patton, G. M., Martin, P. A., Voelker, A., and Salgueiro, E.: Multiproxy comparison of oceanographic temperature during Heinrich Events in the eastern subtropical Atlantic, Earth Planet. Sc. Lett., 310, 45–58, doi:10.1016/j.epsl.2011.07.028, 2011.
Pena, L. D., Calvo, E., Cacho, I., Eggins, S., and Pelejero, C.: Identification and removal of Mn-Mg-rich contaminant phases on foraminiferal tests: implications for Mg/Ca past temperature reconstructions, Geochem. Geophy. Geosy., 6, 9, doi:10.1029/2005GC000930, 2005.
Pena, L. D., Cacho, I., Calvo, E., Pelejero, C., Eggins, S., and Sadekov, A.: Characterization of contaminant phases in foraminifera carbonates by electron microprobe mapping, Geochem. Geophy. Geosy., 9, 7, doi:10.1029/2008GC002018, 2008.
Pierre, C.: The oxygen and carbon isotope distribution in the Mediterranean water masses, Mar. Geol., 153, 41–55, 1999.
Pinardi, N. and Masetti, E.: Variability of the large general circulation of the Mediterranean Sea from observations and modelling: a review, Palaeogeogr. Palaeocl., 158, 153–173, 2000.
Pinot, J. M., López-Jurado, J., and Riera, M.: The CANALES experiment (1996–1998). Interannual, seasonal, and mesoscale variability of the circulation in the Balearic Channels, Prog. Oceanogr., 55, 335–370, 2002.
Piva, A., Asioli, A., Trincardi, F., Schneider, R. R., and Vigliotti, L.: Late-Holocene climate variability in the Adriatic Sea (Central Mediterranean), The Holocene, 18, 153–167, 2008.
Pla, S. and Catalan, J.: Chrysophyte cysts from lake sediments reveal the submillennial winter/spring climate variability in the northwestern Mediterranean region throughout the Holocene, Clim. Dynam., 24, 263–278, 2005.
Pujol, C. and Vergnaud-Grazzini, C.: Distribution patterns of live planktic foraminifers as related to regional hydrography and productive systems of the Mediterranean Sea, Mar. Micropaleontol., 25, 187–217, 1995.
Reguera, M. I.: Respuesta del Mediterráneo Occidental a los cambios climáticos bruscos ocurridos durante el último glacial: estudio de las asociaciones de foraminíferos, PhD Thesis, Dept. of Geology, University of Salamanca, Spain, 2004.
Reimer, P. J., Bard, E., Bayliss, A., Beck, J. W., Blackwell, P. G., Bronk Ramsey, C., Buck, C. E., Edwards, R. L., Friedrich, M., Grootes, P. M., Guilderson, T. P.,

Haflidason, H., Hajdas, I., Hatté, C., Heaton, T. J., Ho_ mann, D. L., Hogg, A. G., Hughen, K. A., Kaiser, K. F., Kromer, B., Manning, S. W., Niu, M., Reimer, R. W., Richards, D. A., Scott, M. E., Southon, J. R., Turney, C. S. M., and van der Plicht, J.: Intcal13 and Marine13 radiocarbon age calibration curves 0–50 000 years cal BP, Radiocarbon, 55, 1869–1887, 2013.

Richter, T. O. and van der Gaast, S.: The Avaatech Core Scanner: technical description and applications to NE Atlantic sediments, in: New Ways of Looking at Sediment Core and Core Data, edited by: Rothwell, R. G., Geological Society Special Publication, London, 39–50, 2006.

Rigual-Hernández, A. S., Sierro, F. J., Bárcena, M. A., Flores, J. A., and Heussner, S.: Seasonal and interannual changes of planktic foraminiferal fluxes in the Gulf of Lions (NW Mediterranean) and their implications for paleoceanographic studies: two 12-year sediment trap records, Deep-Sea Res. Pt. I, 66, 26–40, doi:10.1016/j.dsr.2012.03.011, 2012.

Rigual-Hernández, A. S., Bárcena, M. A., Jordan, R. W., Sierro, F. J., Flores, J. A., Meier, K. J., Beaufort, L., and Heussner, S.: Diatom fluxes in the NW Mediterranean: evidence from a 12-year sediment trap record and surficial sediments, J. Plankton. Res., 35, 5, doi:10.1093/plankt/fbt055, 2013.

Roberts, N., Moreno, A., Valero-Garcés, B. L., Corella, J. P., Jones, M., Allcock, S., Woodbridge, J., Morellón, M., Luterbacher, J., Xoplaki, E., and Türkeş, M.: Palaeolimnological evidence for an east–west climate see-saw in the Mediterranean since AD 900, Global Planet. Change, 84–85, 23–34, doi:10.1016/j.gloplacha.2011.11.002, 2012.

Rodrigo-Gámiz, M., Martínez-Ruiz, S., Rampen, S., Schouten, S., and Sinninghe Damsté, J.: Sea surface temperature variations in the western Mediterranean Sea over the last 20 kyr: a dual-organic proxy ($U^{k'}_{37}$ and LDI) approach, Paleoceanography, 29, 87–98, doi:10.1002/2013PA002466, 2014.

Rogerson, M., Rohling, E. J., Weaver, P. P. E., and Murray, J. W.: The Azores Front since the Last Glacial Maximum, Earth Planet. Sc. Lett., 222, 779–789, doi:10.1016/j.epsl.2004.03.039, 2004.

Rohling, E., Hayes, A., De Rijk, S., Kroon, D., Zachariasse, W. J., and Eisma, D.: Abrupt cold spells in the northwest Mediterranean, Paleoceanography, 13, 316–322, 1998.

Sabatier, P., Dezileau, L., Colin, C., Briqueu, L., Bouchette, F., Martinez, P., Siani, G., Raynal, O., and Von Grafenstein, U.: 7000 years of paleostorm activity in the NW Mediterranean Sea in response to Holocene climate events, Quaternary Res., 77, 1–11, doi:10.1016/j.yqres.2011.09.002, 2012.

Sáez de Cámara, E., Gangoiti, G., Alonso, L., and Iza, J.: Daily precipitation in Northern Iberia: understanding the recent changes after the circulation variability in the North Atlantic sector, J. Geophys. Res., 120, 19, doi:10.1002/2015JD023306, 2015.

Sanchez-Cabeza, J., Masqué, P., and Ani-Ragolta, I.: ^{210}Pb and ^{210}Po analysis in sediments and soils by microwave acid digestion, J. Radioanal. Nucl. Ch., 227, 19–22, 1998.

Schiebel, R., Schmuker, B., Alves, M., and Hemleben, C.: Tracking the Recent and Late Pleistocene Azores front by the distribution of planktic foraminifers, J. Marine Syst., 37, 213–227, 2002.

Schilman, B., Bar-Matthews, M., Almogilabin, A., and Luz, B.: Global climate instability reflected by Eastern Mediterranean marine records during the late Holocene, Palaeogeogr. Palaeocl., 176, 157–176, 2001.

Shackleton, N.: Attainment of isotopic equilibrium between ocean water and the benthonic foraminifera genus *Uvigerina*: isotopic changes in the ocean during the last glacial, CNRS, Colloq. Int., 219, 203–209, 1974.

Sicre, A., Ternois, Y., Miquel, J. C., and Marty, J. C.: Alkenones in the Northwestern Mediterranean sea: interannual variability and vertical transfer, Geophys. Res. Lett., 26, 1735–1738, 1999.

Sicre, M. A., Yiou, P., Eiríksson, J., Ezat, U., Guimbaut, E., Dahhaoui, I., Knudsen, K. L., Jansen, E., and Turon, J. L.: A 4500-year reconstruction of sea surface temperature variability at decadal time-scales off North Iceland, Quaternary Sci. Rev., 27, 2041–2047, doi:10.1016/j.quascirev.2008.08.009, 2008.

Sierro, F. J., Hodell, D. A., Curtis, J. H., Flores, J. A., Reguera, I., Colmenero-Hidalgo, E., Bárcena, M. A., Grimalt, J. O., Cacho, I., Frigola, J., and Canals, M.: Impact of iceberg melting on Mediterranean thermohaline circulation during Heinrich events, Paleoceanography, 20, 1–13, doi:10.1029/2004PA001051, 2005.

Siokou-Frangou, I., Christaki, U., Mazzocchi, M. G., Montresor, M., Ribera d'Alcalá, M., Vaqué, D., and Zingone, A.: Plankton in the open Mediterranean Sea: a review, Biogeosciences, 7, 1543–1586, doi:10.5194/bg-7-1543-2010, 2010.

Sprovieri, R., Stefano, E. Di, Incarbona, A., and Gargano, M. E.: A high-resolution record of the last deglaciation in the Sicily Channel based on foraminifera and calcareous nannofossil quantitative distribution, Palaeogeogr. Palaeocl., 202, 119–142, doi:10.1016/S0031-0182(03)00632-1, 2003.

Steinhilber, F., Beer, J., and Fröhlich, C.: Total solar irradiance during the Holocene, Geophys. Res. Lett., 36, L19704, doi:10.1029/2009GL040142, 2009.

Steinhilber, F., Abreu, J. A., Beer, J., Brunner, I., Christl, M., Fischer, H., Heikkilä, U., Kubik, P. W., Mann, M., McCracken, K. G., Miller, H., Miyahara, H., Oerter, H., and Wilhelms, F.: 9400 years of cosmic radiation and solar activity from ice cores and tree rings, P. Natl. Acad. Sci. USA, 109, 5967–5971, doi:10.1073/pnas.1118965109, 2012.

Stine, S.: Extreme and persistent drought in California and Patagonia during medieval time, Nature, 369, 546–549, 1994.

Stothers, R. B.: Mystery cloud of AD 536, Nature, 307, 344–345, doi:10.1038/307344a0, 1984.

Stuiver, M. and Reimer, P. J.: Extended ^{14}C data base and revised Calib 3.0 ^{14}C age calibration program, Radiocarbon, 35, 215–230, 1993.

Taricco, C., Ghil, M., Alessio, S., and Vivaldo, G.: Two millennia of climate variability in the Central Mediterranean, Clim. Past, 5, 171–181, doi:10.5194/cp-5-171-2009, 2009.

Taricco, C., Vivaldo, G., Alessio, S., Rubinetti, S., and Mancuso, S.: A high-resolution $\delta^{18}O$ record and Mediterranean climate variability, Clim. Past, 11, 509–522, doi:10.5194/cp-11-509-2015, 2015.

Ternois, Y., Sicre, M. A., Boireau, A., Marty, J. C., Miquel, J. C.: Production pattern of alkenones in the Mediterranean Sea, Geophys. Res. Lett., 23, 3171–3174, 1996.

Thornalley, D. J. R., Elderfield, H., and McCave, I. N.: Holocene oscillations in temperature and salinity of the surface subpolar North Atlantic., Nature, 457, 711–714, doi:10.1038/nature07717, 2009.

Thunell, R.C.: Distribution of Recent Planktonic Foraminifera in Surface Sediments of the Mediterranean Sea, Mar Micropaleontol, 3, 147-173, 1978.

Touchan, R., Xoplaki, E., Funkhouser, G., Luterbacher, J., Hughes, M. K., Erkan, N., Akkemik, Ü., and Stephan, J.: Reconstructions of spring/summer precipitation for the Eastern Mediterranean from treering widths and its connection to large-scale atmospheric circulation, Clim. Dynam., 25, 75–98, 2005.

Touchan, R., Akkemik, Ü., Hughes, M. K., Erkan, N.: May–June precipitation reconstruction of southwestern Anatolia, Turkey during the last 900 years from tree rings, Quaternary Res., 68, 196–202, 2007.

Trouet, V., Esper, J., Graham, N. E., Baker, A., Scourse, J. D., and Frank, D. C.: Persistent positive North Atlantic Oscillation mode dominated the Medieval Climate Anomaly, Science, 324, 78, doi:10.1126/science.1166349, 2009.

Trouet, V., Scourse, J. D., and Raible, C. C.: North Atlantic storminess and Atlantic Meridional Overturning Circulation during the last Millennium: reconciling contradictory proxy records of NAO variability, Global Planet. Change, 84–85, 48–55, doi:10.1016/j.gloplacha.2011.10.003, 2012.

Tsimplis, M. N. and Baker, F.: Sea level drop in the Mediterranean Sea: an indicator of deep water salinity and temperature changes?, Geophys. Res. Lett., 27, 1731–1734, 2000.

Tsimplis, M. N. and Josey, S. A.: Forcing of the Mediterranean Sea by atmospheric oscillations over the North Atlantic, Geophys. Res. Lett., 28, 803–806, 2001.

Tsimplis, M. N. and Rixen, M.: Sea level in the Mediterranean Sea: the contribution of temperature and salinity changes, Geophys. Res. Lett., 29, 1–4, doi:10.1029/2002GL015870, 2002.

Vallefuoco, M., Lirer, F., Ferraro, L., Pelosi, N., Capotondi, L., Sprovieri, M., and Incarbona, A.: Climatic variability and anthropogenic signatures in the Gulf of Salerno (southern-eastern Tyrrhenian Sea) during the last half millennium, Rend Lincei, 23, 13–23, doi:10.1007/s12210-011-0154-0, 2012.

van Raden, U. J., Groeneveld, J., Raitzsch, M., and Kucera, M.: Mg/Ca in the planktonic foraminifera Globorotalia inflata and Globigerinoides bulloides from Western Mediterranean plankton tow and core top samples, Mar. Micropaleontol., 78, 101–112, doi:10.1016/j.marmicro.2010.11.002, 2011.

Vargas-Yáñez, M., Moya, F., García-Martínez, M. C., Tel, E., Zunino, P., Plaza, F., Salat, J., and Pascual, J.: Climate change in the Western Mediterranean Sea 1900–2008, J. Marine Syst., 82, 171–176, doi:10.1016/j.jmarsys.2010.04.013, 2010.

Velasco, J. P. B., Baraza, J., and Canals, M.: La depresión periférica y el lomo contourítico de Menorca: evidencias de la actividad de corrientes de fondo al N del Talud Balear, Geogaceta, 20, 359–362, 1996.

Versteegh, G. J. M., de Leeuw, J.W., Taricco, C., and Romero, A.: Temperature and productivity influences on $U^{K'}_{37}$ and their possible relation to solar forcing of the Mediterranean winter, Geochem. Geophy. Geosy., 8, Q09005, doi:10.1029/2006GC001543, 2007.

Villanueva, J., Pelejero, C., and Grimalt, J. O.: Clean-up procedures for the unbiased estimation of C_{37} alkenone sea surface temperatures and terrigenous n-alkane inputs in paleoceanography, J. Chromatogr., 757, 145–151, 1997.

Wallace, J. M. and Gutzler, D. S.: Teleconnections in the geopotential height field during the Northern Hemisphere winter, Mon. Weather Rev., 109, 784–812, 1981.

Wassenburg, J. A., Immenhauser, A., Richter, D. K., Niedermayr, A., and Riechelmann, S.: Moroccan speleothem and tree ring records suggest a variable positive state of the North Atlantic Oscillation during the Medieval Warm Period, Earth Planet. Sc. Lett., 375, 291–302, doi:10.1016/j.epsl.2013.05.048, 2013.

Weldeab, S., Siebel, W., Wehausen, R., Emeis, K., Schmiedl, G., and Hemleben, C.: Late Pleistocene sedimentation in the western Mediterranean Sea: implications for productivity changes and climatic conditions in the catchment areas, Palaeogeogr. Palaeocl., 190, 121–137, 2003.

Wright, H. E.: Global Climates since the Last Glacial Maximum, Minnesota University Press, Minneapolis, 1994.

Yu, J., Elderfield, H., Greaves, M., and Day, J.: Preferential dissolution of benthic foraminiferal calcite during laboratory reductive cleaning, Geochem. Geophy. Geosy., 8, 6, doi:10.1029/2006GC001571, 2007.

Zúñiga, D., García-Orellana, J., Calafat, A., Price, N. B., Adatte, T., Sanchez-Vidal, A., Canals, M., Sanchez-Cabeza, J. A., Masqué, P., and Fabres, J.: Late Holocene fine-grained sediments of the Balearic Abyssal Plain, Western Mediterranean Sea, Mar. Geol., 237, 25–36, 2007.

Table 1. Core tops taken into account in the calibration's adjustment. $\delta^{18}O_c$ and Mg/Ca have been obtained by means of analyses on *G. bulloides* (Mg/Ca procedure have been performed without reductive step).

Core	Location	Latitude	Longitude	Mg/Ca (mmol mol^{-1})	$\delta^{18}O_c$ (VPDB‰)
TR4-157	Balearic Abyssal Plain	40° 30.00' N	4° 55.76' E	3.36	0.53
KTB-34	Cat-Bal Sea (Balears)	40° 27.17' N	3° 43.38' E	4.44	1.05
ALB1	Alboran Sea (WMed)	36° 14.31' N	4° 15.52' W	3.20	0.80
ALBT1	Alboran Sea (WMed)	36° 22.05' N	4° 18.14' W	3.44	0.65
ALBT2	Alboran Sea (EMed)	36° 06.09' N	3° 02.41' W	3.63	0.57
ALBT4	Alboran Sea (EMed)	36° 39.63' N	1° 32.35' W	3.72	0.93
ALBT5	Alboran Sea (EMed)	36° 13.60' N	1° 35.97' W	3.38	0.64

Table 2. Radiocarbon dates obtained on monospecific foraminifer *G. inflata* and calibrated ages, these last one are expressed in years Before Common Era (BCE) and Common Era (CE). MR3.3 dates are presented for the first time in this study. Cores were analysed at the NOSAMS/Woods Hole Oceanographic Institution, USA (OS) and at Direct AMS Radiocarbon Dating Service, USA (D-AMS).

Laboratory Code	Core	Comp. Depth (cm)	^{14}C ages	Cal years BCE/CE (2-σ)
OS-67294	MIN1	7-7.5	895 ± 35	1411 - 1529 CE
OS-67296		19-19.5	2010 ± 35	304 - 544 CE
OS-67291	MIN2	11-11.5	845 ± 35	1440 - 1598 CE
OS-67297		18-18.5	1190 ± 35	1170 - 1312 CE
OS-67324		25-25.5	1540 ± 25	804 - 989 CE
OS-67323		28.5-29	1840 ± 30	520 - 680 CE
D-AMS 004812	MR3.3	3.5-4	938 ± 25	1383 - 1484 CE
OS-87613		6.5-7	1270 ± 35	1063 - 1256 CE
OS-87614		12-12.5	1420 ± 30	911 - 1085 CE
OS-87615		16-17	1900 ± 30	438 - 621 CE
D-AMS 004811		20-21	2350 ± 29	88 BCE - 107 CE
OS-87619		24-25	2620 ± 25	388 BCE - 214 BCE

Table 3. Summary of records analysed and methods utilized in age models.

Core	Records analysed	Age model
MIN1	Mg/Ca-SST, $U^{k'}_{37}$-SST, $\delta^{18}0$	^{14}C, ^{210}Pb, ^{137}Cs, software-simulations, SST-tuning
MIN2	Mg/Ca-SST, $U^{k'}_{37}$-SST, $\delta^{18}0$	^{14}C, ^{210}Pb, software-simulations, SST-tuning
MR3.1A	Mg/Ca-SST, $\delta^{18}0$	^{210}Pb, SST-tuning, geochemical chronostratigraphy, foraminiferal assemblage
MR3.1B	Mg/Ca-SST, $\delta^{18}0$, Geochemical composition	SST-tuning, geochemical chronostratigraphy
MR3.2	Geochemical composition	^{210}Pb, geochemical chronostratigraphy
MR3.3	Mg/Ca-SST, $U^{k'}_{37}$-SST, $\delta^{18}0$,	^{14}C, software-simulations, SST-tuning, foraminiferal assemblage

Table 4. Mean accumulation rates, years covered and mean time resolution of all cores according to final age-depth models.

Core	Mean acc. rate (cm kyr^{-1})	Spanning time (yr)	Mean time resolution (yr cm^{1})
MIN1	14	2528	83
MIN2	25	1538	48
MR3.3	17	2443	78
MR3.1A	15	2635	95
MR3.1B	16	2706	98
MR3.2	15	1797	102

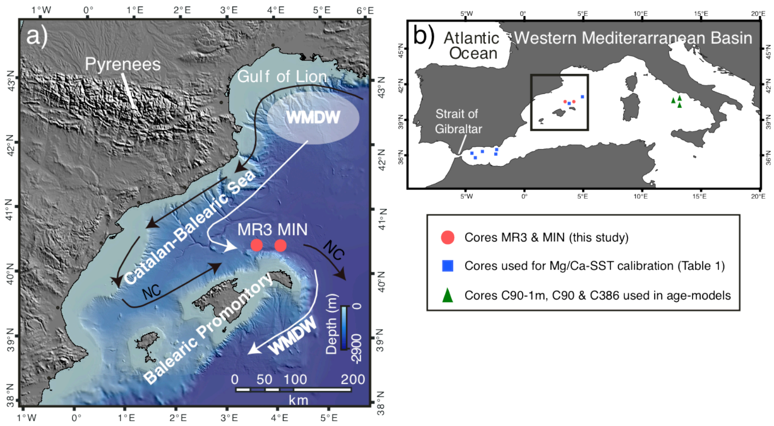

Figure 1. Location of the studied area. (a) Central-western Mediterranean Sea: cores MIN and MR3 effect of this study (red dots) with relevant features of surface (NC: Northern Current) and deep water circulation (WMDW: Western Mediterranean Deep Water). (b) Cores used in age-models development from the Tyrrhenian Sea (green triangles) (Lirer et al., 2013) and cores used in Mg/Ca-SST calibration from the Western Mediterranean Basin (blue squares).

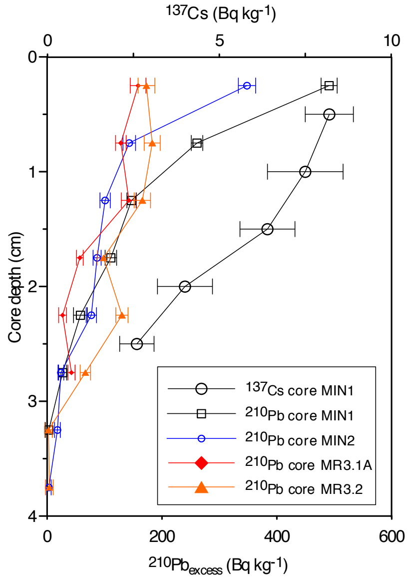

Figure 2. Excess ^{210}Pb (Bq kg^{-1}) profiles for cores MIN1, MIN2, MR3.1A and MR3.2 and also ^{137}Cs concentration profile for core MIN1. Error bars represent 1 σ uncertainty.

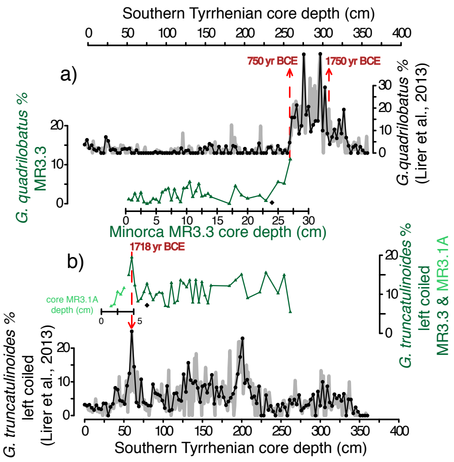

Figure 3. Comparison among the quantitative distribution patterns of (a) *G. quadrilobatus* and (b) *G. truncatulinoides* left coiled with core MR3.3 (dark green plot) and data from the composite core (C90-1m, C90 and C836 cores) studied in the southern Tyrrhenian Sea (Lirer et al., 2013), expressed as 3 point average and with the grey area corresponding to the entire record. The two tie points used in age models (dashed red line) correspond to 1718 yr CE and 750 yr BCE. Black diamonds show ^{14}C dates from core MR3.3.

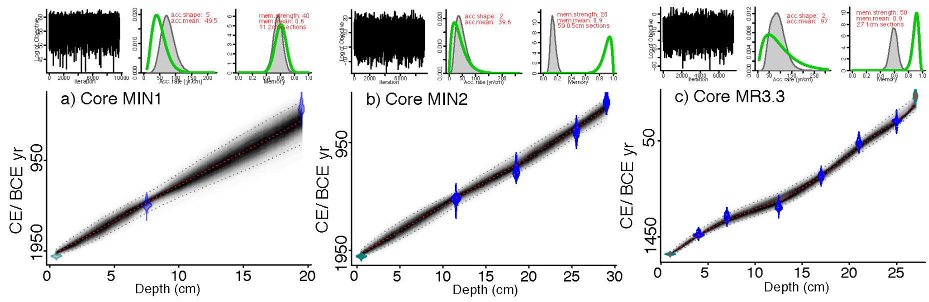

Figure 4. Age-depth models based on Bayesian accumulation simulations (Blaauw and Christen, 2011): (a) core MIN, (b) MIN2 and (c) MR3.3. The three upper plots in each core show the stable MCMC run achieved (left), the prior (green line) and posterior (grey) distributions of the accumulation rates (middle), and the prior (green line) and posterior (grey) distributions of the memory (right). Each main graphic represents the age–depth model for each core (darker grey indicates more probable calendar ages) based on the prior information, the calibrated radiocarbon dates (purple symbols), sample year for cores MIN (blue symbols) and biostratigraphical dates from core MR3.3 (red symbols).

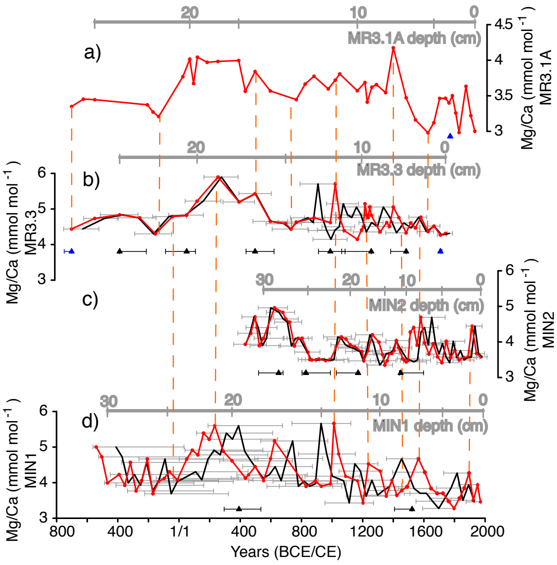

Figure 5. Main procedures of multy-proxy chronostratigraphy performed with Mg/Ca records for cores: (a) MR3.1A, (b) MR3.3, (c) MIN2 and (d) MIN1. Final age-depth models are plotted in red. Black plots and grey error bars correspond to Bayesian accumulation age-depth models. Triangles represent to ^{14}C dates (black) and biostratigraphical dates based on planktonic foraminifera (blue), and they are shown below the corresponding core and with their associated 2 σ errors. Depths in relation to the final age model can be observed above its corresponding core. Vertical dashed lines (orange) indicate tie points between the different Mg/Ca records (tie points and attendant uncertainties in Table S1 of Supplementary Information).

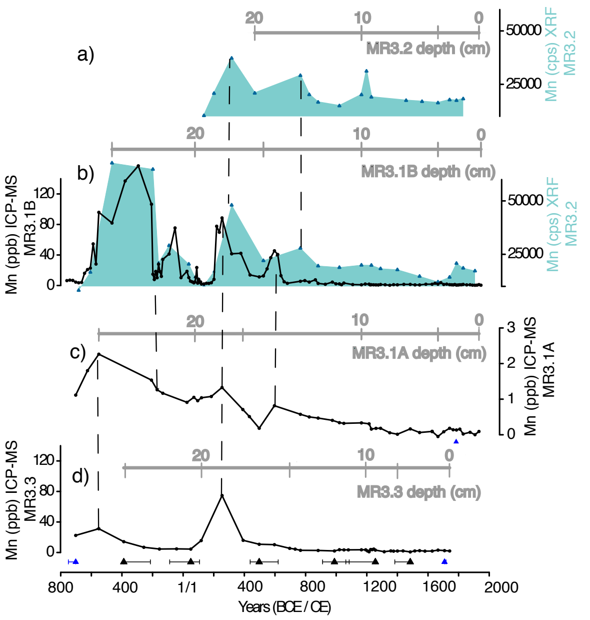

Figure 6. Multy-proxy chronostratigraphy performed with Manganese profiles. Blue filled plots represents Mn profiles obtained by XRF Core-Scanner for cores (a) MR3.2 and (b) MR3.1B, respectively. Black plots show Mn from trace elements analysed by means of ICP-MS for cores (b) MR3.1B, (c) MR3.1A and (d) MR3.3. Vertical dashed lines indicate tie points of geochemical chronostratigraphy (tie points and attendant uncertainties in Table S1 of Supplementary Information). Triangles represent to ^{14}C dates (black) and biostratigraphical dates based on planktonic foraminifera (blue) and they are shown below the corresponding core and with their associated 2 σ errors.

Comentario [1]: axis b) (right) it's wrong. MR3.2 should be MR3.1B. It will be modified.

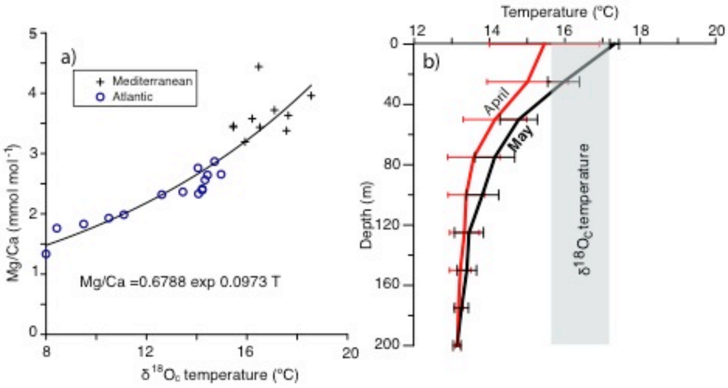

Figure 7. (a) Exponential function and correlation obtained between $\delta^{18}O_c$ temperatures and Mg/Ca for western Mediterranean Sea. ± 0.7°C is the standard error in calibrations on all the *G.bulloides* core tops utilized in this paper from the north-western Mediterranean Sea (see Table 1) and it is consistent with ± 0.6°C obtained for the Atlantic Ocean in Elderfield and Ganssen (2000) and also ± 1.1°C in the same sp. culture data (Lea et al., 1999). (b) April (red) and May (black) temperature profiles of the first 200 m measured during years 1945-2000 in stations corresponding to the studied core tops (MEDAR GROUP, 2002). In grey is shown the $\delta^{18}O_c$ average temperature of all cores.

Comentario [2]: Figures will be changed in order to include uncertainties on both the pre-exp and exp

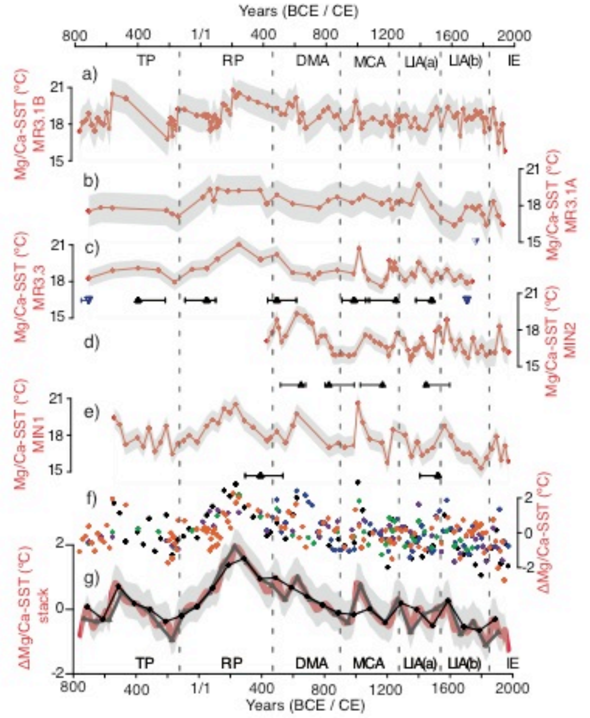

Comentario [3]: Figure will be modified after the different trace element data treatment applied.

Figure 8. SST obtained by means of analysis of Mg/Ca for cores: (a) MR3.1B, (b) MR3.1A, (c) MR3.3, (d) MIN2 and (e) MIN1. Grey-scales integrate the reproducibility in Mg/Ca concentrations in each analysis and ± 0.7°C, which is the calculated standard error in *G. bulloides* core top calibrations for the central-western Mediterranean Sea developed in this paper. (f) All individual SST anomalies on their respective time step (MR3.1B: orange, MR3.1A: purple, MR3.3: green, MIN2: blue and MIN1: black dots). (g) 20 yr cm^{-1} stacked temperature anomaly (red plot) with its 2σ uncertainty (grey band). The 80 yr cm^{-1} (grey plot) and the 100 yr cm^{-1} (black plot) stacks are also shown. Triangles represent to ^{14}C dates (black) and biostratigraphical dates based on planktonic foraminifera (blue) and they are shown below the corresponding core and with their associated 2 σ errors.

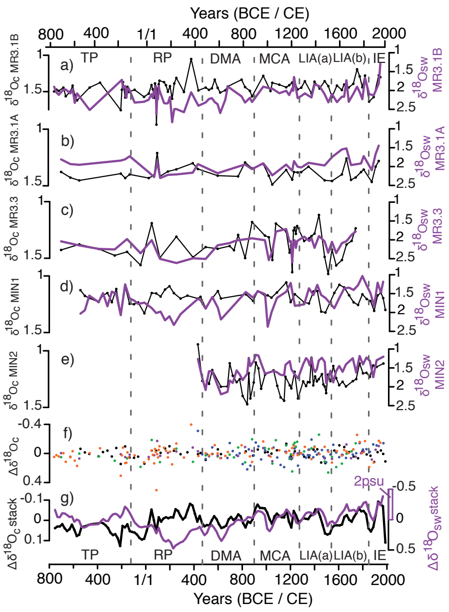

Figure 9. Oxygen isotope measured on carbonates shells of *G. bulloides* ($\delta^{18}O_c$ VPDB‰, in black) and their derived $\delta^{18}O_{SW}$ (purple) for cores: (a) MR3.1B, (b) MR3.1A, (c) MR3.3 (d) MIN2 and (e) MIN1. (f) Individual $\delta^{18}O_c$ (VPDB‰) anomalies on their respective time step. (g) Both respective anomaly stacked records and the equivalence between $\delta^{18}O_{SW}$ (SMOW‰) and salinity, calculated according to Pierre (1999). It is estimated that the rise of one unit of $\delta^{18}O_{SW}$ would amount to an enhancement of 4 practical salinity units.

Comentario [4]: Figure will be modified after the different trace element data treatment applied.

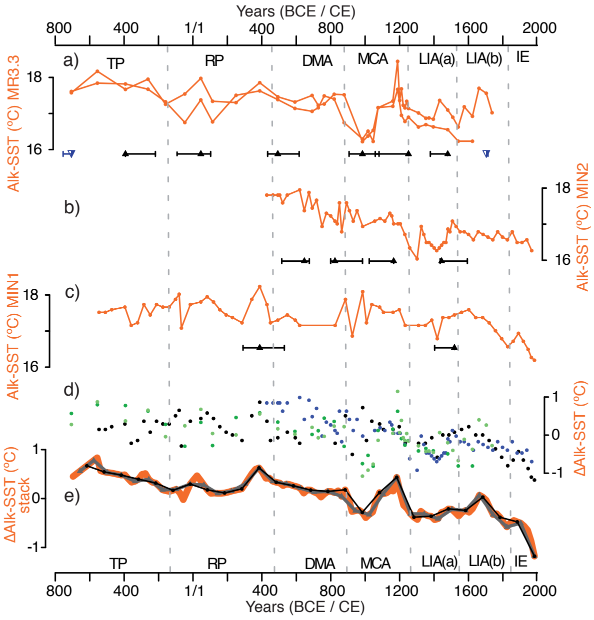

Figure 10. Alkenone temperature records from Minorca (this study) for cores: (a) MR3.3, (b) MIN2 and (c) MIN1. Triangles represent to ^{14}C dates (black) and biostratigraphical dates based on planktonic foraminifera (blue) and they are shown below the corresponding core and with their associated 2σ errors. (d) All individual alkenone derived SST anomalies on their respective time step (MR3.3: green, MIN2: blue and MIN1: black dots); (e) 20 yr cm^{-1} stacked temperature anomaly (orange plot). The 80 yr cm^{-1} (grey plot) and the 100 yr cm^{-1} (black plot) stacks are also shown.

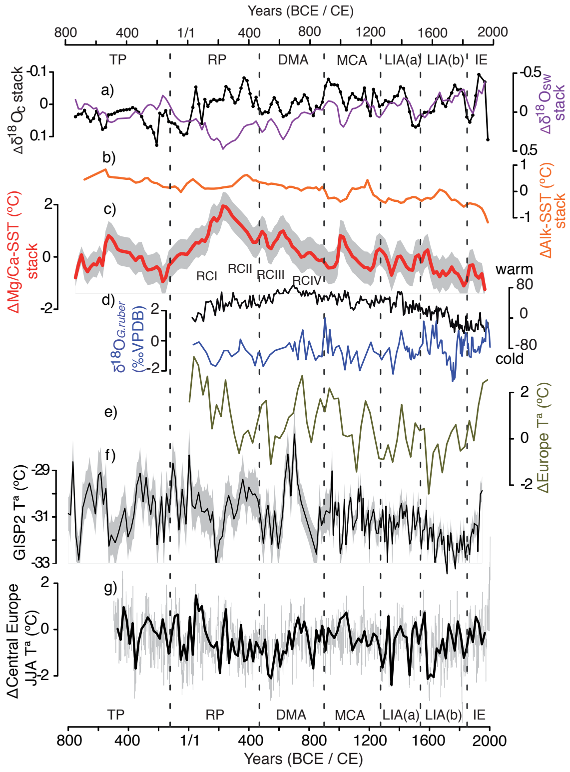

Figure 11. Temperature and isotope anomaly records from Minorca (this study) and data from another regions. (a) $\delta^{18}O_c$ (VPDB‰) and $\delta^{18}O_{SW}$ (SMOW‰) Minorca stacks, (b) Alkenone-SST anomaly Minorca stack, (c) Mg/Ca-SST anomaly Minorca stack, (d) warm and cold phases and $\delta^{18}O_{G.ruber}$ recorded by planktonic foraminifera from the southern Tyrrhenian composite core, respectively and RCI to RCIV showing roman cold periods (Lirer et al., 2014), (e) 30-year averages of the PAGES 2k Network (2013) Europe anomaly Temperature reconstruction, (f) Greenland snow surface temperature (Kobashi et al., 2011) and (g) Central Europe Summer anomaly temperature reconstruction in Central Europe (Büntgen et al., 2011).

Comentario [5]: Figure will be modified after the different trace element data treatment applied.

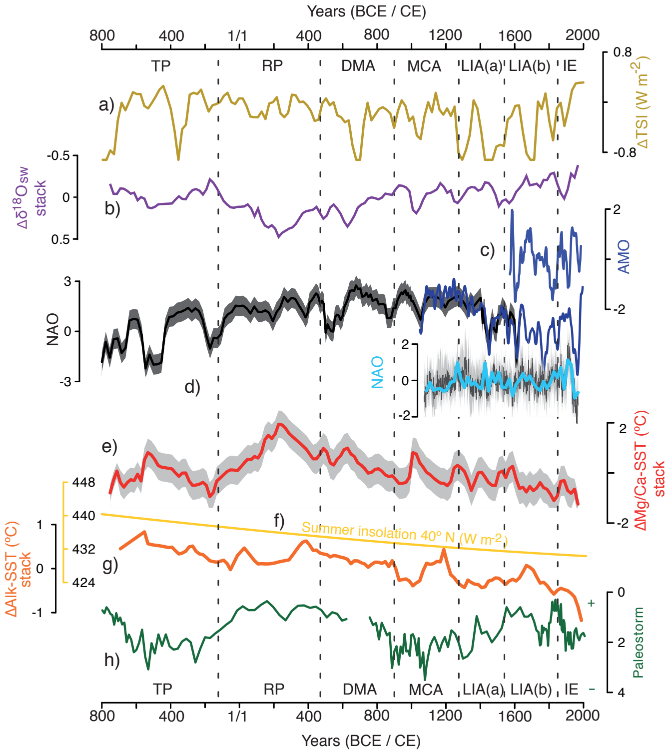

Figure 12. Temperature and isotope anomaly records from Minorca (this study) and data from another regions and with external forcings: (a) Total Solar Irradiance (Steinhilber et al., 2009, 2012), (b) $\delta^{18}O_{SW}$ Minorca stacks, (c) Atlantic Multidecadal Oscillation (AMO) (Gray et al., 2004), (d) North Atlantic Oscillation (NAO) reconstructions (Olsen et al., 2012, Trouet et al., 2009, and for the last millennium: Ortega et al., 2015), (e) Mg/Ca-SST anomaly Minorca stack, (f) Summer Insolation at 40 °N (Laskar et al., 2004), g) Alkenone-SST anomaly Minorca stack and (h) Paleostorm activity in the Gulf of Lions (Sabatier et al., 2012).

Comentario [6]: Figure will be modified after the different trace element data treatment applied.

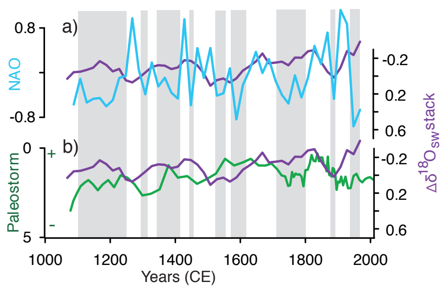

Figure 13. $\delta^{18}O_{SW}$ Minorca stack during the last millennium (age is expressed in years Common Era) plotted with (a) NAO reconstruction (Ortega et al., 2015) and (b) Paleostorm activity in the Gulf of Lion (Sabatier et al., 2012).

Comentario [7]: The proposed changes in scales will be done (Fig. 13a).

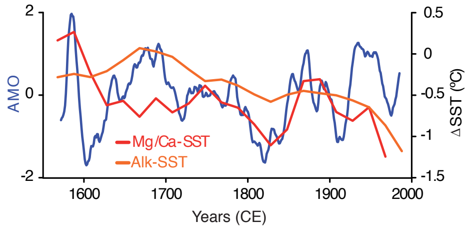

Figure 14. Mg/Ca-SST and Alkenone-SST Minorca anomaly stacks during the last centuries plotted with AMO reconstruction (Gray et al., 2004).